

Ocean Acidification: Net Ecosystem Calcification Response to an Elevated pCO₂ Level

A THESIS SUBMITTED TO THE GLOBAL ENVIRONMENTAL SCIENCE
UNDERGRADUATE DIVISION IN PARTIAL FULFILLMENT OF THE
REQUIREMENTS FOR THE DEGREE OF

BACHELOR OF SCIENCE

IN

GLOBAL ENVIRONMENTAL SCIENCE

MAY 2007

By

Adrian Thomas Lee Tan

Thesis Advisors

Fred T. Mackenzie
Jane E. Schoonmaker

We certify that we have read this thesis and that, in our opinion, it is satisfactory in scope and quality as a thesis for the degree of Bachelor of Science in Global Environmental Science.

THESIS ADVISORS

Fred T. Mackenzie
Department of Oceanography

Jane E. Schoonmaker
Department of Oceanography

Acknowledgements

I would like to thank my thesis advisors: Fred T. Mackenzie and Jane E. Schoonmaker for their unconditional support and infinite patience. Needless to say my graduation was only made possible by their willingness to go above and beyond for their students. The completion of this thesis could never have been done without the assistance of Andreas Andersson to whom I will be eternally grateful. I am extremely fortunate to have met, and worked with such a true advocate of science. One could only hope to gain the knowledge and fortitude Andreas reflects in his work.

I would also like to thank Rene Tada and Kathy Kozuma for their guidance while I enjoyed my stay in the GES program. Their supervision created a sense of home in the department.

Professors, colleagues, and peers that deserve mention for making life in the GES program interesting, fun, rewarding, and memorable are Eric De Carlo, Michael Guidry, Laura Degelleke, Christopher Colgrove, Rachel Solomon, Whitney Hassett, and Megan O'Brian. Each individual mentioned has carved a lasting memory in my life.

Finally I would like to thank my family: Tommy Tan, Margaret Tan, Bernice Tan, Melissa Tan, Linda Cua, Adam Cua, Kathy Cua, Jackie Cua, and Sasha Cua for supporting my education and providing me a home filled with an atmosphere of love. No son, brother, nephew, or cousin could ever ask for more.

Abstract

Ocean acidification is the lowering of seawater pH due to increased pCO₂ levels in the atmosphere brought about by human activities of fossil fuel burning and deforestation. As of 2005 atmospheric pCO₂ levels had reached 380 ppm (IPCC, 2007), the highest level for the last 640,000 years (Petit et al., 1999; Barnola et al., 2003, Siegenthaler et al., 2005, IPCC, 2007). The increase in pCO₂ in the atmosphere is an immediate concern because of its direct relationship with ocean chemistry. The change in ocean chemistry due to the addition of CO₂ lowers both the pH and saturation state of seawater with respect to different CaCO₃ minerals (Andersson et al., 2003, Morse et al., 2006). Calcification rates decrease as the saturation state of seawater with respect to CaCO₃ decreases, hence producing weaker skeletons for calcareous organisms. The weaker coralline structures lead to greater vulnerability to physical and biological erosion.

A diurnal study of the effects of increased pCO₂ levels in the atmosphere on calcification rates of corals was done using a flow through mesocosm in which the coral *Montipora capitata* was grown. The experiment quantitatively compared the calcification rates of corals in tanks with an elevated CO₂ level of 700 ppm (projected atmospheric CO₂ level by the year 2100) to those of tanks with ambient CO₂ levels (380 ppm). Net ecosystem calcification (NEC) rates were calculated using total alkalinity (TA) and pH measurements of water flowing in and out of the tanks. The results of this experiment showed that an elevated CO₂ level of ~700 ppm induced a significant reduction in net calcification rates compared to NEC in the tanks with

ambient CO₂ levels. The calculations of NEC showed average net dissolution rates over a diurnal cycle for tanks with elevated CO₂ levels.

Table of Contents

Acknowledgements	iii
Abstract	iv
List of Table and Figures	vii
Chapter 1 – Introduction	1
1.1 – Global Warming	1
1.2 – Ocean Acidification	8
1.3 – Carbonate Chemistry of Seawater	10
1.4 – CO ₂ Flux Determinants	12
1.4.1 – CO ₂ Physical Response	12
1.4.2 – Calcification and Dissolution	12
1.4.3 – Photosynthesis and Respiration	14
1.5 – Objectives of this Study	15
Chapter 2 – Experimental Setup and Analytical Methodology	17
2.1 – Experimental Setup	17
2.2 – Experimental Tank Measurements	19
2.3 – Laboratory Analysis	20
2.3.1 – DIC	20
2.3.2 – Total Alkalinity	20
2.3.3 – Carbonate Species Calculation	21
2.4 – Nature of Samples	21
Chapter 3 – Results	22
Chapter 4 – Calculations and Discussion of Results	27
4.1 – pH-TA vs. pH-O ₂ Method (pH-TA Method Validity)	27
4.2 – Calculation of Net Ecosystem Calcification Rates	30
4.3 – Discussion of Results	32
Chapter 5 - Conclusions	36
Appendix A: SRES	39
Appendix B: Data: Measurements from Ocean Acidification Experiment	40
Appendix C: Calculations for NEC	42
References	44

List of Table and Figures

<u>Table</u>		<u>Page</u>
1	Proposed functions of calcification by different organisms.....	13
 <u>Figures</u>		
1	Measured and past prediction of global and continental temperature change.....	2
2	Monthly mean pCO ₂ levels measured at the Mauna Loa Observatory.....	3
3	Trends in atmospheric CO ₂ , CH ₄ , and δD from 640 Kya to present from the Vostok ice core.....	4
4	Historical and projected global warming from 1900 to 2100.....	5
5	Correlation between sunspot cycle lengths and the mean northern hemisphere temperature record between 1861 to 1989.....	6
6	Global mean radiative forcing summary.....	7
7	Historical and projected saturation state of seawater with respect to different carbonate minerals.....	9
8	Aerial photograph of the University of Hawaii Institute of Marine Biology, Moku o Lo'e, Oahu, Hawaii.....	18
9	Control and experimental tanks used in calcification experiment.....	19
10	pH, DO, and temperature of the system throughout the 24-hour ocean acidification experiment.....	23
11	Total alkalinity of the system during the 24-hour ocean acidification experiment.....	24
12	HCO ₃ ⁻ , CO ₃ ²⁻ , CO ₂ , and total carbon of the system throughout the 24-hour ocean acidification experiment.....	25
13	Aragonite and calcite saturation states throughout the 24-hour ocean acidification experiment.....	26
14	Total alkalinity box model of the ocean acidification experiment.....	30

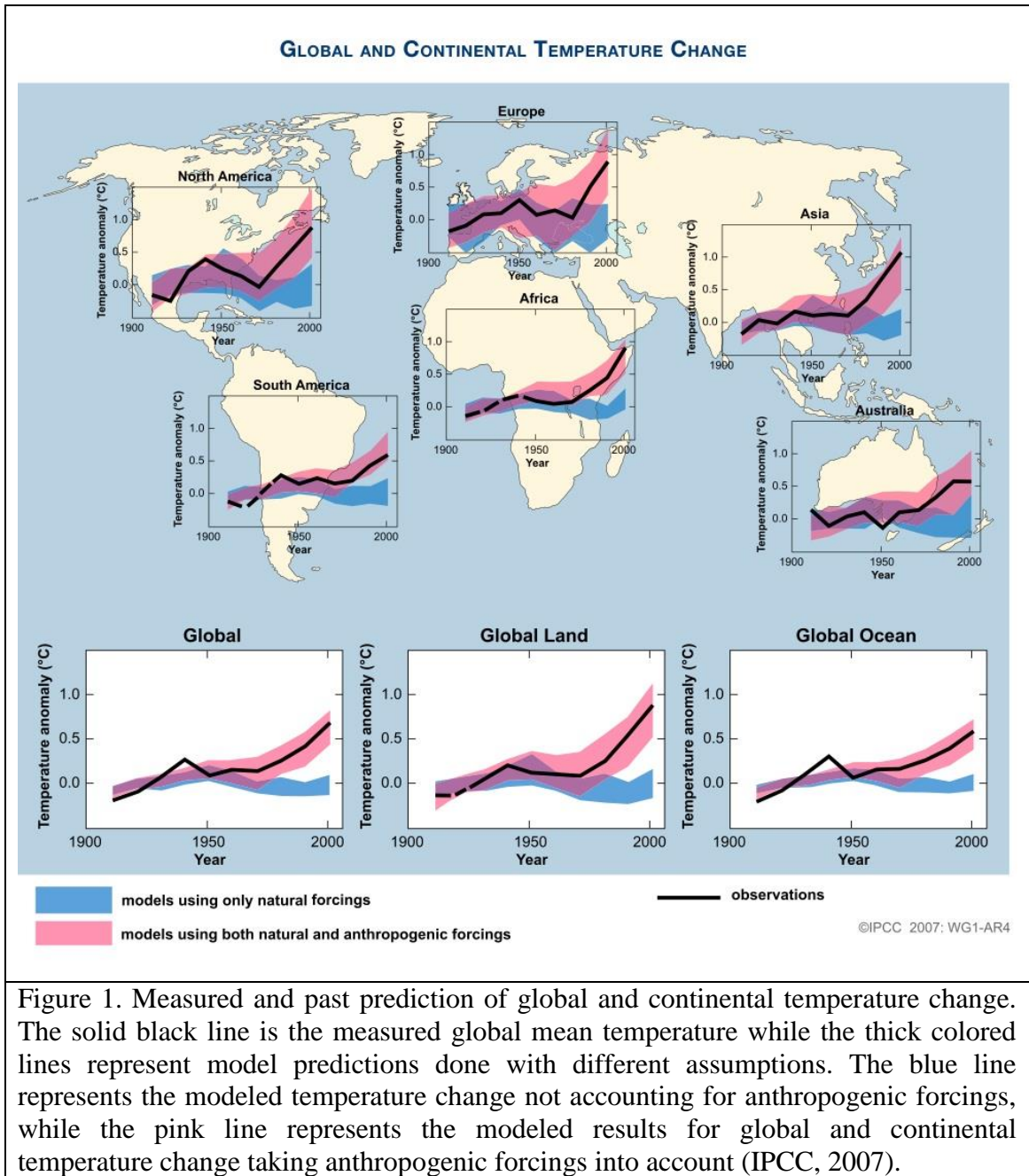
15	Net ecosystem calcification rate throughout the 24-hour ocean acidification experiment.....	33
16	Average net ecosystem calcification rate throughout the 24-hour ocean acidification experiment.....	34

Chapter 1 – Introduction

1.1 – Global Warming

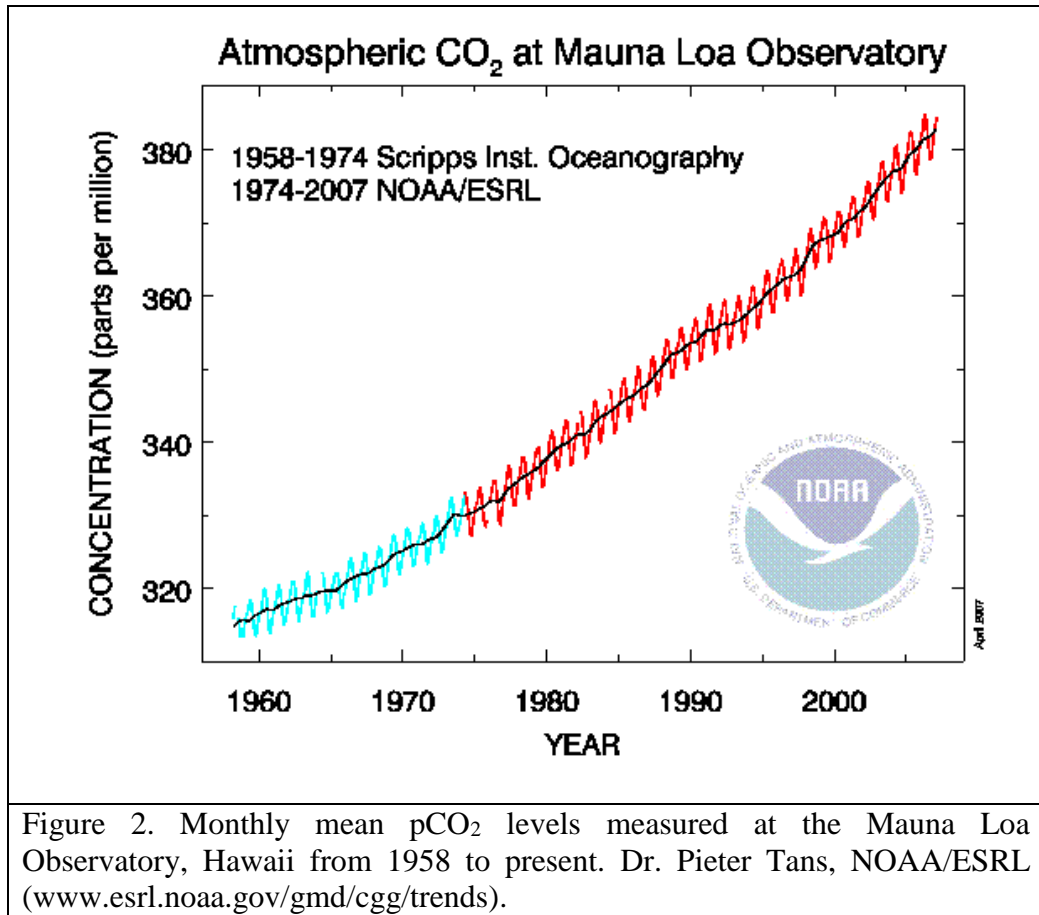
Global warming today is a real concern with real consequences. Figure 1 shows how global and continental temperatures changed from 1906 to 2005. The figure compares actual global and continental temperature change to model predictions with natural and anthropogenic forcings. This figure shows how the change in global temperature is very close to model predictions that account for anthropogenic forcing. Anthropogenic forcing in the model is mostly driven by the increase in atmospheric CO₂ from fossil fuel burning (Solomon, 2007). CO₂ is a major gas of concern for global warming and should closely be monitored.

As of 2005 atmospheric pCO₂ concentrations were at 380 ppmv (IPCC, 2007). Figure 2 shows the steady increase of pCO₂ in the atmosphere from 1958 to present. The annual CO₂ concentration growth rate from 1995 to 2005 was 1.9 ppmv, which is considerably higher than the average growth rate from 1960 to 2005 of 1.4 ppmv per year (IPCC, 2007). Houghton (2001) showed that atmospheric pCO₂ levels could reach 970 ppmv by the end of the 21st century depending on factors like population growth, economic growth, technological development, and environmental protection. Models show that if atmospheric pCO₂ stabilized at 750 ppmv in the year 2100, it would still take more than a thousand years for temperature and sea levels to return to preindustrial values (Solomon, 2007).



According to the analysis of the trapped gas bubbles in Antarctic ice cores (Figure 3), present values of $p\text{CO}_2$ are the highest concentrations observed in 640,000 years (Petit et al., 1999; Barnola et al., 2003; Siegenthaler et al. STET 2005; IPCC, 2007). This is alarming because the Special Report on Emission Scenarios (SRES) models from

the IPCC with different degrees of conservatism all show a distinct increasing trend in global surface temperature likely driven by CO₂ from anthropogenic sources (Figure 4).



The model projections show that if CO₂ emissions were held at year 2000 values, a temperature increase of 0.1 °C per year would be expected; however, if CO₂ emissions increased to IPCC SRES values, an increase of 0.2 °C per year would be expected (IPCC, 2007). According to Houghton et al (2001), a 1.4° to 5.8° C in temperature is expected by the end of the 21st century.

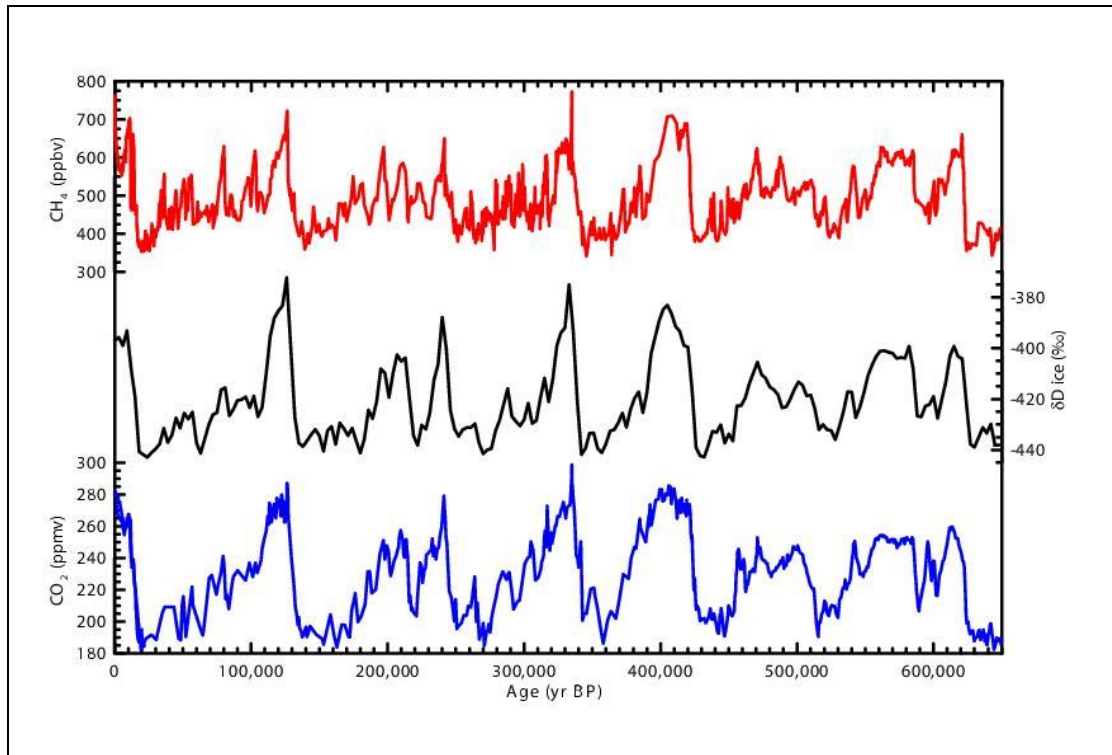


Figure 3. Trends in atmospheric CO₂, CH₄, and δD from 640 Kya to present from the Antarctic ice cores. The figure shows the correlation between CO₂ and temperature (δD). The record indicates that during this time period CO₂ values never exceeded the present value. (www.realclimate.org)

CO₂ levels in the atmosphere have a very strong correlation with temperature; however, it is still not certain that the increased pCO₂ in the atmosphere is the main cause of the warming of the earth. According to the ice core record, the temperature increase of the earth has a lag with relation to the pCO₂ increase in the atmosphere (Petit et al., 1999). There is growing evidence that celestial processes (Figure 5) such as solar and cosmic ray activity also may play a role in regulating the earth's temperature (Friis-Christensen and Lassen, 1991; Svensmark 1998). Continuous monitoring of total solar irradiance now covers the last 28 years (Solomon, 2007). The data show a well established 11-year cycle in irradiance that varies by 0.08% from solar cycle minima to maxima, with no significant long-term trend (Solomon, 2007). The primary known cause of contemporary irradiance variability is the presence of sunspots (compact, dark features

where radiation is locally depleted) and faculae (extended bright features where radiation is locally enhanced) (Solomon, 2007). Estimated direct radiative forcing due to changes in solar output since 1750 is $+0.12$ [$+0.06$ to $+0.03$] W/m^2 , far less than the radiative forcing of CO_2 in the atmosphere (>1.5 W/m^2).

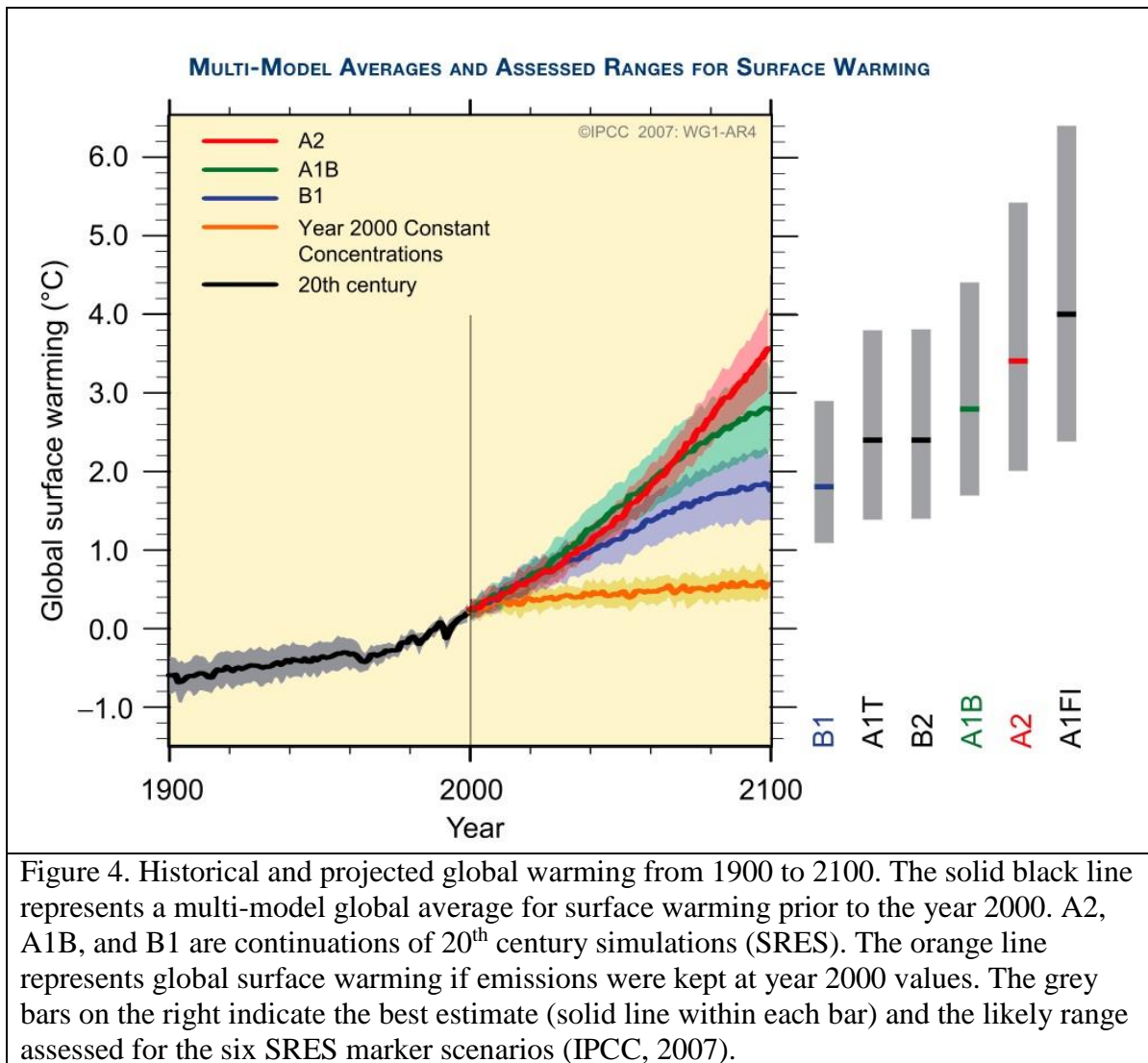


Figure 4. Historical and projected global warming from 1900 to 2100. The solid black line represents a multi-model global average for surface warming prior to the year 2000. A2, A1B, and B1 are continuations of 20th century simulations (SRES). The orange line represents global surface warming if emissions were kept at year 2000 values. The grey bars on the right indicate the best estimate (solid line within each bar) and the likely range assessed for the six SRES marker scenarios (IPCC, 2007).

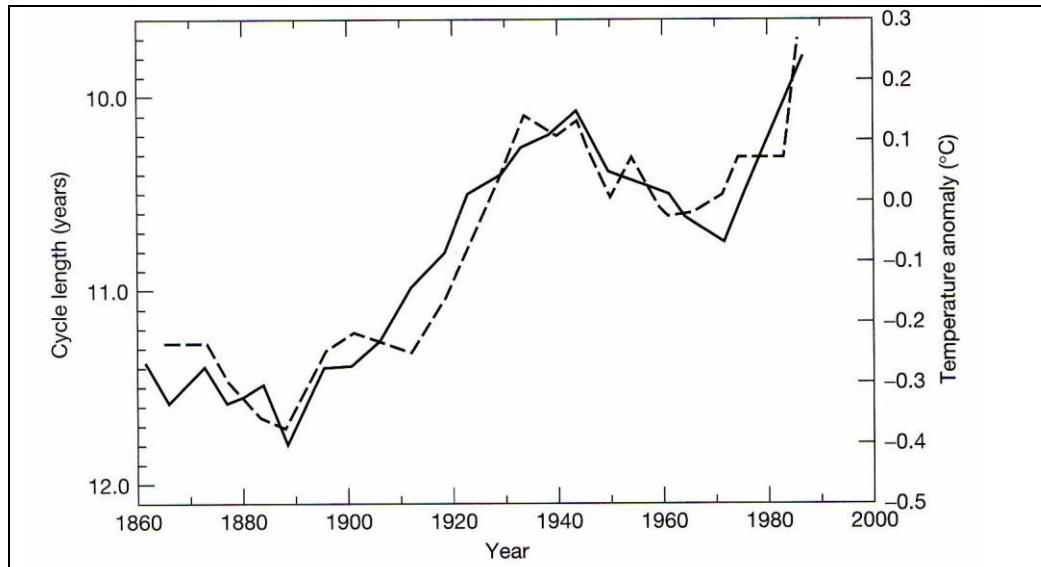


Figure 5. Correlation between sunspot cycle lengths (solid line) and the mean northern hemisphere temperature record between 1861 to 1989 (Friis-Christensen and Lassen, 1991; Svensmark and Solanki, 2002).

Figure 6 summarizes the different radiative forcings (RF) that affect the earth's mean global temperature. Factors that affect RF are: long lived greenhouse gasses, ozone, water vapor from CH₄, surface albedo, aerosols, and solar irradiance (Solomon, 2007). By accounting for these RF factors, it can clearly be seen that anthropogenic radiative forcing outweighs that of the natural RF. The greatest contributor for RF is CO₂, which is mostly of anthropogenic origin. The increasing concentrations of CO₂ in the atmosphere lead to global warming and ocean acidification.

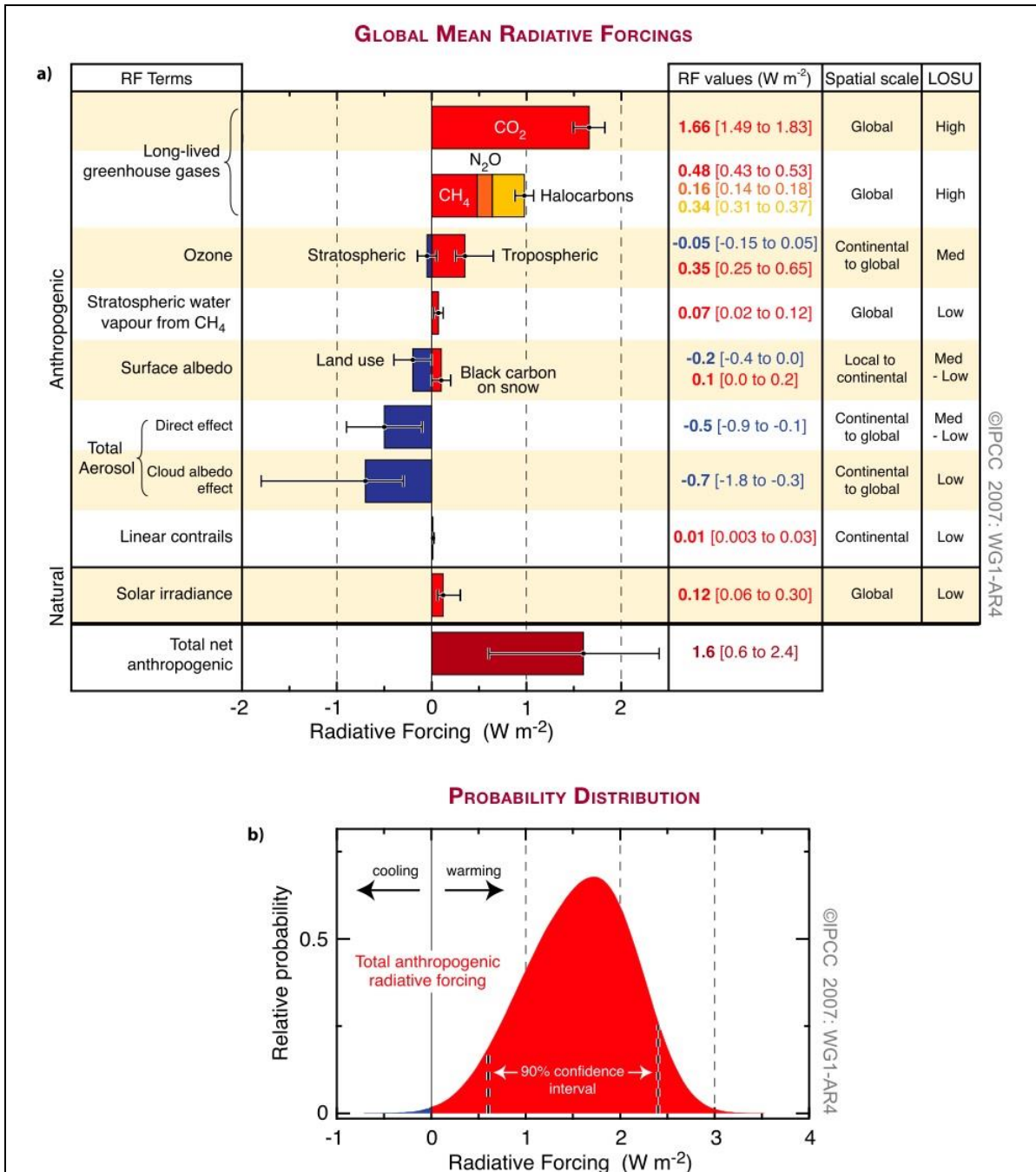
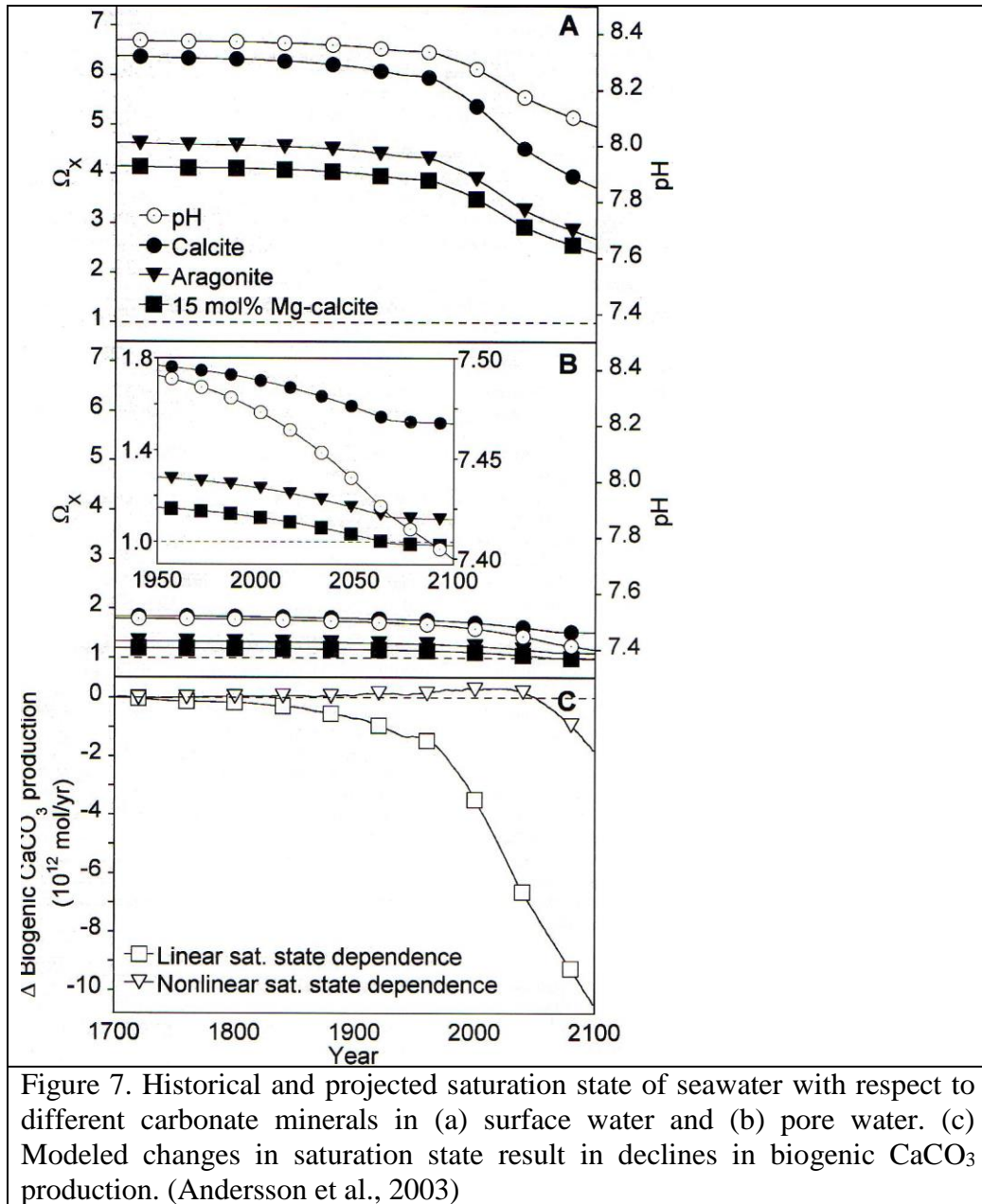


Figure 6. Global mean radiative forcing (RF) summary. (a) Shows all the factors that contribute to global mean RF. Factors include both natural and anthropogenic forcings. The forcings labeled red contribute to global warming, while forcings labeled blue oppose global warming. (b) Probability distribution of the global mean combined RF from all anthropogenic agents shown in (a). Distribution is calculated by combining the best estimates and uncertainties of each component (Solomon, 2007).

1.2 – Ocean Acidification

The ocean is the largest labile reservoir for carbon on decadal to millennial timescales. The ocean acts as a variable sink for atmospheric $p\text{CO}_2$ and other climate-relevant trace gasses (Siegenthaler and Sarmiento, 1993). $p\text{CO}_2$ in the atmosphere would be much higher if not for the ocean acting as a carbon sink. At present, roughly 50% of the anthropogenic CO_2 in the atmosphere is transported to the ocean by physical processes (Sabine et al., 2004, Morse et al., 2006). Estimates of the ocean CO_2 uptake for the last 20 years amount to 1/3 of the CO_2 released from fossil fuel burning alone (Prentice et al., 2001). Models suggest that on millennial timescales the ocean will be the ultimate sink for about 90% of the anthropogenic carbon released to the atmosphere (Archer et al., 1998). However, the ocean cannot be regarded as an unlimited sink for anthropogenic carbon. Under future greenhouse warming climate scenarios, the ocean's physical uptake capacity of anthropogenic carbon is expected to decline. This decline is due to surface warming, increased vertical stratification, and possibly a slowed thermohaline circulation (Sarmiento et al., 1998).

The increase in $p\text{CO}_2$ in the atmosphere is of great concern because of its direct relationship with ocean chemistry. As $p\text{CO}_2$ in the atmosphere increases from fossil fuel emissions and other anthropogenic sources of CO_2 , the ocean consequently takes up more CO_2 , hence changing its chemistry with poorly known consequences for marine life (Kleypas et al., 2006, Morse et al., 2006). The change in water chemistry lowers the pH and saturation state of seawater with respect to different CaCO_3 minerals (Figure 7) (Andersson et al., 2003, Morse et al., 2006).



Calcification rates decrease as seawater carbonate saturation states decrease (Figure 7c). Lowered calcification rates may cause the production of weaker calcareous skeletons and greater vulnerability to physical erosion for calcifying organisms leading to unhealthy and unstable reefs. In addition to increased susceptibility to physical erosion, as the coralline structure gets weaker, macrobioerosion (mollusks and sponges) and

microbioerosion (fungi and microalgae) may play an even more pronounced role in the ecosystem (Kleypas et al., 2006).

Alternatively, it has been suggested that projected changes in seawater chemistry will not significantly affect marine calcifiers. This is due to the argument that any changes in saturation state and pH will be restored by dissolution of metastable carbonate minerals (Halley and Yates, 2000; Barnes and Cuff, 2000). However, according to numerical models done by Andersson et al. (2003), reactions in marine porewaters are not able to buffer the entire water column. Andersson's model suggests dissolution of metastable carbonate phases within the porewater-sediment system will not generate enough total alkalinity to buffer the pH or carbonate saturation state of the entire water column.

1.3 – Carbonate Chemistry of Seawater

The dissolved inorganic carbon (DIC) chemistry in seawater is complex in that CO₂ reacts to produce carbonic acid and other dissolved inorganic carbon species. The distribution of inorganic carbon species in a system is a function of temperature, salinity, and pressure. Increases in atmospheric pCO₂ will lead to more CO₂ invasion to the ocean, hence increasing the DIC in the mixed layer of the ocean. Consequently, CO₃²⁻ concentrations will decrease, lowering the saturation state of seawater with respect to carbonate minerals (Andersson et al., 2003). The following equations represent the DIC system reactions (Morse and Mackenzie, 1990):





The ocean contains 50 times more inorganic carbon than the atmosphere. There are 3 pools of oceanic DIC: HCO_3^- (90%), CO_3^{2-} (9%), and dissolved CO_2 (1%) (Gattuso et al., 1999). CO_2 in surface waters is close to equilibrium with the atmosphere. Calcification is coupled with the DIC system. The carbon atom that is incorporated in the production of CaCO_3 is from HCO_3^- .



H^+ ions are released in the process of calcification hence making seawater more acidic. The additional acid pushes HCO_3^- across into the oceanic CO_2 pool.



Physical equilibrium between the oceanic and atmospheric CO_2 pools determines whether the flux of CO_2 is to or from the ocean (Gattuso et al., 1999). The DIC system is important in seawater chemistry in that it functions as a buffer for seawater pH on time scales of up to several thousand years (Pilson, 1998).

The removal of DIC, redistribution of the dissolved carbonate species, and changes in the relative concentration of CO_2 in solution are controlled significantly by the precipitation of CaCO_3 mineral phases and biological production of organic matter (Lerman and Mackenzie, 2005). The rates at which these factors change affect the CO_2 flux across the air-sea interface. According to the stoichiometry of Equation 7 for calcification, precipitation of calcium carbonate will raise the pCO_2 of the system while

dissolution lowers it. This ultimately may lead to changes in the CO₂ concentrations in other reservoirs (Lerman and Mackenzie, 2005). Over glacial-interglacial timescales, preservation and dissolution of CaCO₃ in ocean sediments act to maintain a nearly constant ocean alkalinity that provides a significant negative feedback on changes in atmospheric pCO₂ (Archer, 1996).

1.4 – CO₂ Flux Determinants

1.4.1 – CO₂ Physical Response

Shallow water ocean environments, i.e. bays, estuaries, lagoons, banks, and continental shelves, constitute ~7% of global ocean surface area, but are the source of 10-30% of the world's marine primary production (Gattuso et al., 1998). These regions are important with respect to the carbon flux because 85% of the organic carbon and 45% of the inorganic carbon in the ocean are buried in shallow water ocean sediment environments. According to Andersson and Mackenzie (2004), the net flux of CO₂ between the ocean and the atmosphere is dependent in part on the partial pressure gradient between the two. Calcification, dissolution, photosynthesis, and respiration influence the partial pressure gradient and thus also play major roles in determining the net flux of CO₂.

1.4.2 – Calcification and Dissolution

Calcification evolved sometime during the Cambrian period, coincident perhaps with a sudden rise in Ca²⁺ (e.g. Kleypas et al., 2006). Since high concentrations of Ca²⁺ are toxic to cellular processes, it has been proposed that calcification may have been the detoxification mechanism at the time (Brennan et al., 2004). Organisms since then have

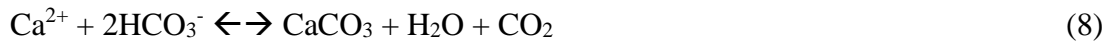
harnessed this evolutionary process to produce CaCO_3 shells and skeletons for protection and other functions (Table 1). Predictions of how reduced calcification rates will affect different organisms are based on the assumption that calcification serves multiple functions that benefit different species (Kleypas et al., 2006).

Table 1. Proposed functions of calcification by different organisms (Kleypas et al., 2006)

Function	Planktonic	Benthic
Protection	all groups	all groups
Buoyancy regulation	coccolithophores, foraminifera	
Light modification	coccolithophores	corals
Provide protons for conversion of HCO_3^- to CO_2 for photosynthesis	coccolithophores	calcareous algae?
Facilitate bicarbonate-based photosynthesis	coccolithophores	
Aid in capture of prey	foraminifera	
Reproduction	foraminifera, some pteropod species	corals?
Prevention of osmotically induced volume changes	coccolithophores	
Extension into hydrodynamic regime		corals, calc. algae, bryozoans
Anchoring to substrate		corals, calc. algae, bryozoans
Competition for space		corals, calc. algae, bryozoans

Calcification is a CO_2 -releasing process that can make seawater initially in equilibrium with the atmosphere degas against the initial pCO_2 gradient (Ware et al., 1992). In this respect, most coral reefs are actually CO_2 sources and not CO_2 sinks (Ware et al., 1992). Coral reef building requires that calcification exceeds dissolution so that any growing coral reef system is a net source of CO_2 , hence contributing to greenhouse gasses in the atmosphere. This is a positive feedback, until a certain threshold, for coral growth because according to Mackenzie and Agegian (1989), the rate of calcification of coralline algae and corals exhibits a strong positive correlation to saturation state and a negative parabolic dependence on temperature, a statement documented in numerous other experiments.

The precipitation of CaCO₃ minerals from supersaturated water is accompanied by a decrease in total alkalinity and an increase in dissolved CO₂ and H⁺ ion concentration, which results in a lowering of the seawater pH (Lerman and Mackenzie, 2005). Equation 8 shows the stoichiometry of calcification. The forward reaction denotes precipitation while the backward reaction denotes dissolution.



The equation shows the relationship between calcification, CO₂ production, and total alkalinity. Calcification removes two moles of carbon from solution and produces one mole of CO₂, while dissolution consumes CO₂ and produces HCO₃⁻. Two equivalents of TA are produced for every mole of CaCO₃ dissolved.

1.4.3 – Photosynthesis and Respiration

Primary production consumes CO₂ and respiration of organic matter produces CO₂. Equation 9 shows the stoichiometry of photosynthesis and respiration. The forward reaction denotes gross primary production while the backward reaction denotes autorespiration.



The main site for marine calcification is the euphotic zone (upper ~50 m of ocean water) where calcifying organisms (phytoplankton, zooplankton, zoobenthos) thrive (Lerman and Mackenzie, 2005). In euphotic zones where the gross primary production greatly exceeds autorespiration, the removal of CO₂ may essentially compete with carbonate precipitation that generates CO₂ that can be emitted to the atmosphere (Equation 8) (Lerman and Mackenzie, 2005). Some of the calcium carbonate produced in surface

coastal and open ocean water dissolves in the water column and in sediments. These dissolution reactions are driven by CO₂ produced during remineralization of sinking organic matter deposited in sediments that produces CO₂ (Emerson and Bender, 1981). This process results in the return of carbon taken up in calcification and organic matter production back to ocean water as alkalinity and DIC, respectively.

The dissolution of CaCO₃ in reef environments is expected to increase in response to ocean acidification. Net carbonate dissolution is observed in many reef environments at night (Kleypas et al., 2006). This occurs when respiration greatly increases and elevates the local pCO₂ of the water column. Dissolution is likely to be occurring all the time in the sediments and carbonate framework of reefs; however, it is only evident at night when it is not masked by a higher rate of carbonate precipitation (Kleypas et al., 2006). In a strongly autotrophic ecosystem, CO₂ production by calcification may be counteracted by organic productivity through uptake of the generated CO₂, resulting in lower CO₂ transfer rates from the ocean to the atmosphere, or ultimately a reversal (Lerman and Mackenzie, 2005).

1.5 – Objectives of this Study

It is anticipated that increased acidification of the oceans from uptake of CO₂ will result in decreased calcification rates of marine organisms (e.g., Kleypas et al., 2006). The extent of reduction of calcification rates as a function of pCO₂, however, is not well characterized. In addition, although some calcifying organisms are known to undergo dissolution at night, they are net calcifiers on a diurnal basis under current oceanic saturation states. It is not known how much CO₂ is required to force a calcifying system to a state of net dissolution on a diurnal basis. The objective of this study was to

investigate the effects of ocean acidification on coral calcification rates. Specifically, experiments were designed to quantify the calcification rates over a 24-hour cycle of corals exposed to two different levels of pCO₂.

A mesocosm experiment using two sets of tanks with different pCO₂ levels was conducted to compare the net ecosystem calcification rate of a system with a raised pCO₂ level of ~700 ppm (experimental tank) with that of a system with an ambient pCO₂ level of 380 ppm (control tank). My hypothesis is that the difference in pCO₂ levels of the control and experimental tanks will be significant enough to cause a distinct decline in net ecosystem calcification rates for the experimental tank.

Chapter 2 – Experimental Setup and Analytical Methodology

2.1 – Experimental Setup

A diurnal study of the effects of increased pCO₂ levels in the atmosphere on calcification rates of coral was done at the Hawaii Institute of Marine Biology in Moku O Lo'e (Coconut Island), Southern Kaneohe Bay, Hawaii (Figure 8). Six fiberglass tanks of 0.5 m³ (1 x 1 x 0.5 m) were flushed with running seawater (~8 L min⁻¹) directly pumped from the edge of the coral reef (Figure 9). The experimental design involved growth of a single species of coral (*Montipora capitata*) in a series of flow-through mesocosms. Inflow waters in half of the mesocosms were manipulated to increase artificially pCO₂ levels. The carbonate chemistry of the inflow and mesocosm tank waters was monitored, and the differences were used to calculate rates of calcification in each of the mesocosms. The experiment started at 12:00 noon on June 22, 2006 and ended at 12:00 noon the next day.

The residence time of the water in the tanks was approximately 1 hour. All of the tanks had corals of the same species and comparable sizes (see section 2.4). Three tanks were used as experimental tanks for manipulation of seawater pCO₂. Concentrated hydrochloric acid (HCl) mixed with fresh water to a 10% solution was added to the seawater flowing into the experimental tanks. The acid was added using a 205CA Watson Marlow multichannel peristaltic pump at a rate of 1.3 ml min⁻¹ through 2.05 mm tubing. HCl added to the system shifted the distribution of dissolved carbonate species, increasing the pCO₂. The resulting seawater was equivalent to that in equilibrium with an atmosphere having a pCO₂ of 745 ± 130 ppmv. This CO₂ level is slightly lower than the

expected pCO₂ levels in the end of the 21st century following a business as usual (BAU) scenario (Houghton et al., 1996, 2001). In the remaining three control tanks, fresh water was added at the same rate as HCl was added to the experimental tanks. Measurements of temperature, pH, and dissolved oxygen (DO) in all six tanks were taken in two hour increments, while samples for salinity, total alkalinity (TA) and dissolved organic carbon (DIC) were taken every four hours. The experimental setup was the same as that used by Kuffner et al. (in press) and Rodgers et al. (in press). The data from this experiment are shared between all authors.



Figure 8. Aerial photograph of the University of Hawaii Institute of Marine Biology, Moku o Lo'e, Oahu, Hawaii. (Photograph taken from Coconut Island Website - <http://www.hawaii.edu/HIMB/>)



Figure 9. Control and experimental tanks used in calcification experiment under present and elevated CO₂ conditions located at the University of Hawaii Institute of Marine Biology, Moku o Lo'e, Oahu, Hawaii. (Photograph courtesy of Ku'ulei Rodgers of Hawaii Institute of Marine Biology)

2.2 – Experimental Tank Measurements

Temperature and salinity were measured in each tank using a YSI 30 salinity/conductivity/temperature meter with accuracies of ± 0.1 °C and ± 0.1 ppt, respectively. Dissolved oxygen was measured using a YSI 95 Dissolved Oxygen Microelectrode Array Model with an accuracy of ± 0.2 mg L⁻¹. The pH of each tank was measured using a fully enclosed Oakton Ag/AgCl combination electrode attached to an Accumet AP72 handheld pH/mV/temperature meter with an accuracy of ± 0.01 pH units. The pH electrode was calibrated using 4.00 and 7.00 NBS buffer solutions from Fisher Scientific (± 0.01 pH units @ 25 °C). Water samples for total alkalinity were collected of surface seawater in each tank using 200 mL Kimax brand glass sample bottles and were poisoned with a saturated solution of mercuric chloride (HgCl₂). 100 μ L of HgCl₂ solution were added to each sample. Each bottleneck was taped with Teflon tape prior to sampling to assure a

tight seal and prevent atmospheric equilibration of gasses. Dissolved inorganic carbon samples were collected in a similar manner to alkalinity (Kuffner et al., in press).

2.3 – Laboratory Analyses

2.3.1 – DIC

Seawater samples collected for DIC were analyzed using a Li-Cor 6262 NDIR as a detector. Unfortunately the DIC results could not be used in the interpretations described in this paper. This was due to the fact that the sample bottles were not stored properly and CO₂ was exchanged with the atmosphere.

2.3.2 – Total Alkalinity

Collected seawater samples for total alkalinity were titrated using the potentiometric acid titration (DOE, 1994). The system was modified by Dr. Rolf Arvidson of Rice University, Houston, Texas during his affiliation with the University of Hawaii. The alkalinity driver routine (GranPlot) and the fitting routine (GranFit) were modified to be able to adjust the “Gran boundary”, “Gran pts”, and “Gran pts to fit” to obtain a precision of 0.15%. The Gran pts and boundaries are internal parameters of the program to adjust for precision and accuracy of the titration. The Accumet calomel combo electrode was attached to an Orion expandable ion analyzer EA920. The Brinkmann Metrohm Dosimat was used to dispense 0.1 M HCl for titrations. Both apparatuses were remotely controlled by a GranPlot driver. The 0.1 M HCl acid was standardized against certified reference material (CREM) prepared by Andrew Dickson at Scripps Institution of Oceanography. CREMs were analyzed after every 7th sample

determination to ensure accuracy and precision of the titration. Titrations were accurate and precise to less than 1% error.

2.3.3 – Carbonate Species Calculation

The carbonate species were calculated using the CO2SYS software program (Lewis and Wallace, 1998). The CO₂ system parameters were calculated at *in situ* temperature and salinity from total alkalinity and pH employing stoichiometric carbonic acid system constants calculated on the NBS scale by Peng et al. (1987) based on the constants defined by Mehrbach et al. (1973).

2.4 – Nature of Samples

The seawater chemistry in both the control and experimental tanks was given four weeks to stabilize prior to the introduction of coral colonies. Two sets of *Montipora capitata* colonies of comparable size (~10 cm diameter) and morphology were collected. The two colonies were collected at similar depths off Moku O Lo'e Island. One colony came from the windward flat reef, and the other at the fringing reef south of the island. Twenty colonies from the two sets were randomly picked and placed in the experimental and control tanks (Rodgers, in press).

Chapter 3 – Results

Results of the diurnal experiment as described in Chapter 2 are summarized in the figures below. Figure 10 shows the pH (Figure 10a), dissolved oxygen (DO) (Figure 10b), and temperature (Figure 10c) of each of the tanks. Symbols in blue represent the control tanks (8, 10, 12) and symbols in red represent the experimental tanks (7, 9, 11). The dashed line represents the input characteristics of the seawater from Kaneohe Bay, and reflects the natural external variance of the parameters being measured.

The pH of the system falls at night owing to the lack of photosynthesis and reduced calcification. As photosynthesis decreases and respiration increases at night, the amount of CO_2 in solution increases, hence lowering the pH of the system. Equation 6 (calcification equation) shows that for every mole of CaCO_3 produced, 1 mole of H^+ is also produced, hence further lowering the pH of the system. However, the reduced calcification at night implies less protons produced by this reaction. In addition, photosynthesis releases O_2 during the day, and respiration uses up O_2 at night. As can be seen in Figure 10, photosynthesis plays an important role in the system. As would be predicted, the temperature of the system is the lowest before daybreak at about 6 am and the highest past noon at about 2 pm. This is because water has a high specific heat and therefore heats up slowly, and conversely releases heat slowly as well.

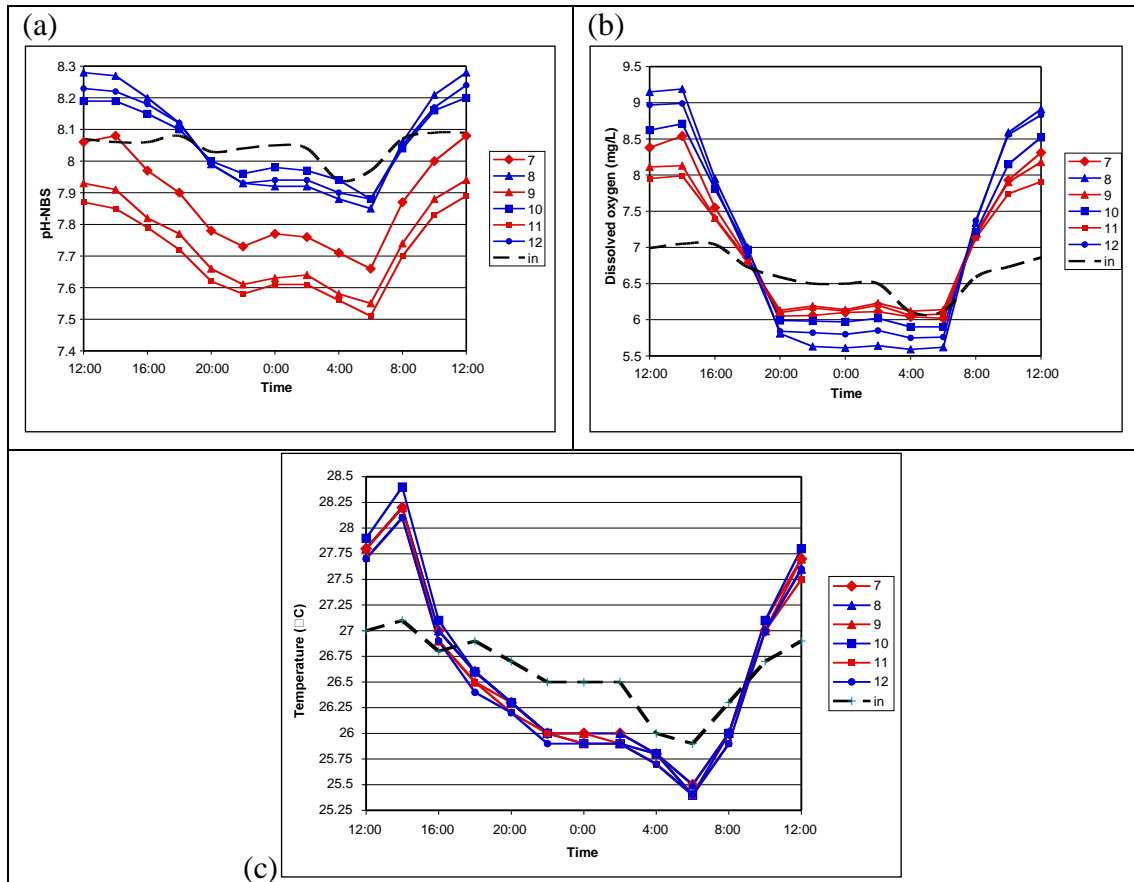


Figure 10. pH, DO, and temperature of the system throughout the 24-hour ocean acidification experiment. (a) The pH of the system decreases at night when respiration exceeds photosynthesis and releases more CO_2 to the system. (b) DO decreases at night when respiration exceeds photosynthesis and uses up the available DO in the system. (c) Temperature of the system fluctuates with respect to the temperature variance of night and day. The dashed line represents the input solution, which is seawater pumped directly from Kaneohe bay.

The total alkalinity (TA) of the system behaves as predicted. As can be seen in Figure 11, TA is lowest during the day. This is due to the calcification process using up free HCO_3^- in the system (Equation 6). The reduction of free HCO_3^- in the system causes TA to decrease.

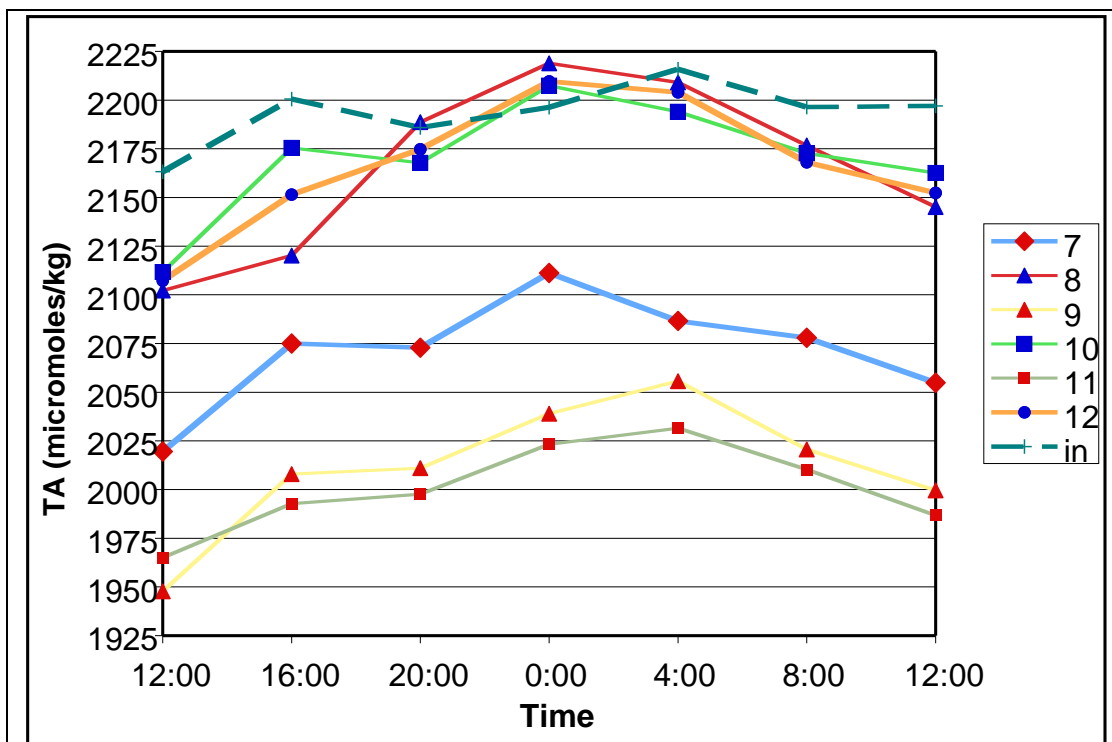


Figure 11. Total alkalinity of the system during the 24-hour ocean acidification experiment. Total alkalinity is controlled by the uptake and release of HCO_3^- in the system through calcification. As more calcification occurs, more HCO_3^- is used. Calcification is prominent during the day hence the lower TA.

The carbonate system is closely tied to photosynthesis/respiration and calcification/dissolution processes. Figure 12c shows how CO_2 increases at night via respiration, and decreases during the day via photosynthesis. Through the DIC equations (Equations 1 to 5), it can be seen that as more CO_2 is added to a system, HCO_3^- (Figure 12a) is produced. CO_3^{2-} (Figure 12b) decreases at night because H^+ ions react with it to produce more HCO_3^- . This leads to the fluctuation in the concentration of HCO_3^- with respect to time. The graph shows this pattern perfectly. Changes in the total carbon (TC) of the system (Figure 12d) are also driven by photosynthesis and calcification. At night when respiration is greater than photosynthesis, CO_2 is produced contributing to more TC in the system. Calcification at night is at a minimum hence less HCO_3^- in solution (Equation 8) is taken from the water, further increasing the TC of the system.

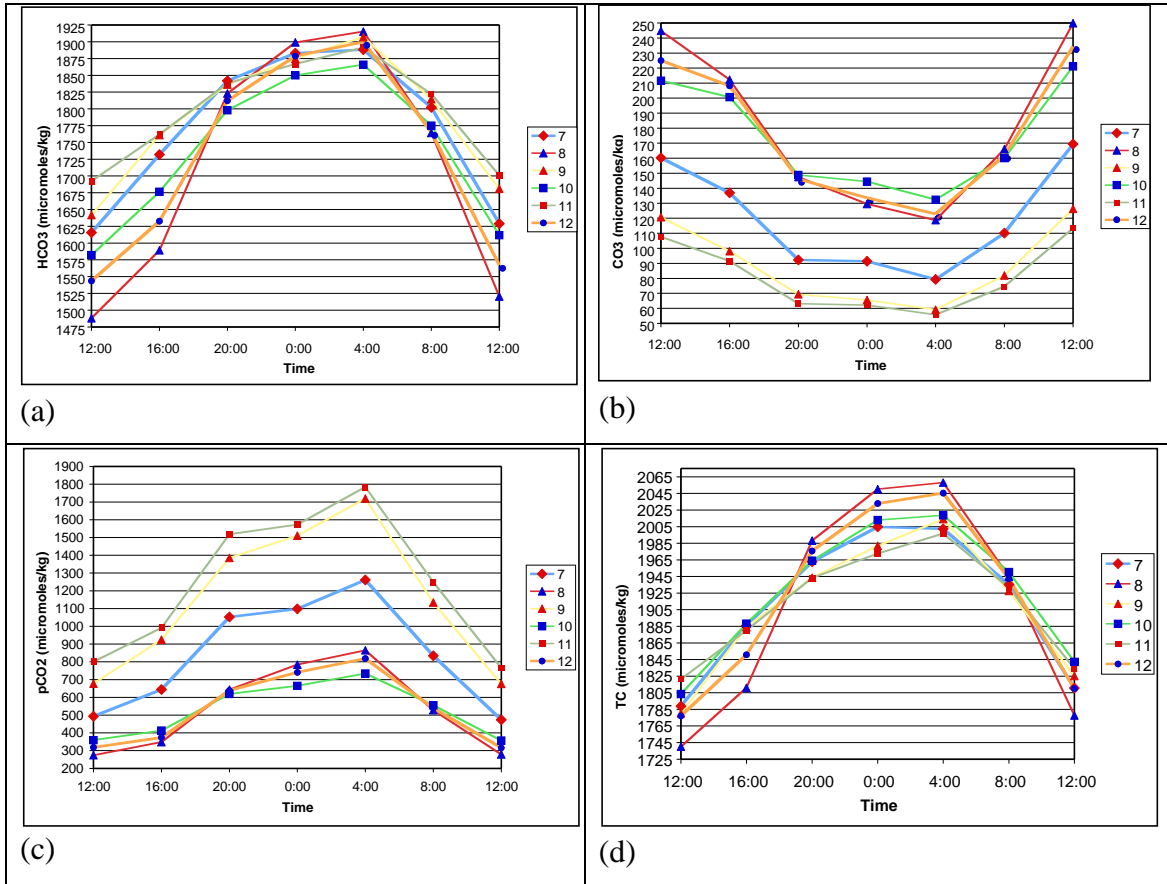


Figure 12. HCO_3^- , CO_3^{2-} , CO_2 , and total carbon of the system throughout the 24-hour ocean acidification experiment. (a) HCO_3^- increases at night when more is produced via the increase of CO_2 in the system from respiration. (b) CO_3^{2-} decreases at night when CO_2 increases producing more H_2CO_3 , which dissociates to produce HCO_3^- . (c) CO_2 rises at night due to the increase of respiration. (d) The total carbon of the system is dependent on photosynthesis and respiration, and calcification and dissolution which dictate the addition and removal of CO_2 , driving the DIC in either direction.

The saturation state of seawater with respect to (a) aragonite and (b) calcite (Figure 13) is defined here as the product of the concentrations of dissolved Ca^{2+} and carbonate ions divided by their product at equilibrium.

$$([\text{Ca}^{2+}] \times [\text{CO}_3^{2-}]) / K_{\text{CaCO}_3} = \Omega \quad (10)$$

When $\Omega = 1$, the solution is saturated with respect to CaCO_3 . When Ω exceeds 1 then the solution is supersaturated. Ω less than 1 denotes undersaturation of seawater with respect

to CaCO_3 . As CO_2 is added to the system, more H^+ ions are released. The excess H^+ ions combine with CO_3^{2-} hence producing more HCO_3^- . Figure 13 shows how the saturation states for both aragonite and calcite decrease at night when excess CO_2 is added to the system through respiration, and increase during the day when photosynthesis exceeds respiration hence reducing CO_2 . As seen in Figure 13, the increase in pCO_2 in the experimental tanks (red symbols) results in lower saturation states with respect to both calcite and aragonite relative to conditions in the control tanks (blue).

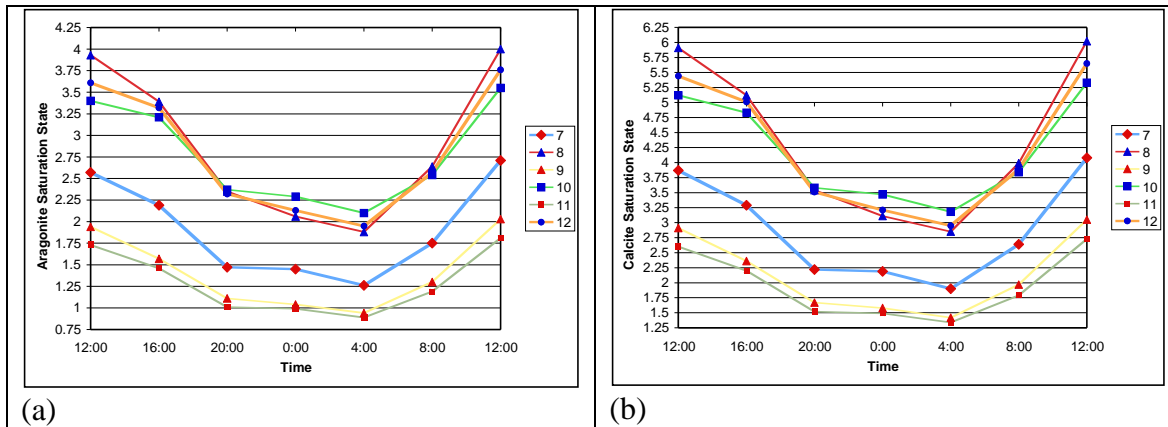


Figure 13. Aragonite and calcite saturation states throughout the 24-hour ocean acidification experiment. (a) Aragonite and (b) calcite saturation states decrease at night when CO_2 from respiration increases. The increase in CO_2 releases H^+ ions, hence lowering pH. The H^+ ions react with CO_3^{2-} hence lowering the saturation state.

CHAPTER 4 – Calculations and Discussion of Results

4.1 – pH-TA vs. pH-O₂ method (pH-TA Method Validity)

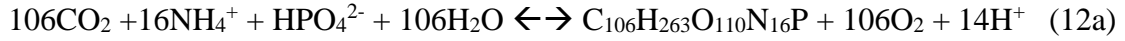
There are two tested methods to measure community metabolism as described by Gattuso et al. (1999), the pH-TA method and the pH-O₂ method. The pH-TA method deals with values of pH in a given system measured continuously and the total alkalinity, which is measured at discrete time intervals. The fact that TA cannot be measured instantaneously gives rise to criticism of the use of this method. The pH-TA method is based on measurements of pH and total alkalinity upstream (input) and downstream (output) of a community. The measurements are then used to calculate the difference between the upstream and downstream concentrations of dissolved inorganic carbon (Δ DIC) using stoichiometric equations that describe the seawater carbonate system. Equation 11 is used to calculate the rate of calcification using TA and calcification relationships.



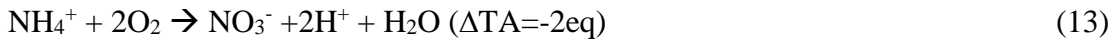
However, a 1:1 molar relationship between CO₂ and CaCO₃ only holds true for freshwater. The ratio is lower for seawater because of its buffering capacity (Frankignoulle, 1994).

A major assumption to keep in mind in the pH-TA method is the assumption that there is no process other than calcification that significantly affects TA, and that the removal and addition of CO₂ from photosynthesis and respiration do not play a role in the TA calculations. However, photosynthesis and respiration are coupled with assimilation and dissimilation of NH₄⁺, NO₃⁻, and HPO₄²⁻, which liberate OH⁻ or H⁺ (or uptake H⁺ or

OH⁻) as shown in equations 12a and 12b. The forward reactions for Equations 12a and 12b represent photosynthesis as written and respiration is in the reverse direction.



Nitrification and sulfate reduction reactions alter the TA of a system more significantly as shown in equations 13 and 14.



However, this does not invalidate the method, because as shown by Kinsey (1978), the summation of equations 11 to 14 is likely to cause less than a 5% error in the net calcification rates calculated for specific reefs. A bigger potential problem with the pH-TA method is that organic acids can significantly contribute to TA in euphotic environments (Cai and Wang, 1998), but concentrations of organic acids in reef settings are not overly high. A study by Cai and Wang (1998) shows that the organic acid alkalinity behaves conservatively in organic rich estuaries in Georgia. This is a reasonable assumption for ocean water as well because the DOC is comparable, and ocean water has a much lower concentration of organic acids. Also, because TA measurements in community metabolism deal with changes in TA over time (not absolute values), the effects are negligible. Finally, the validity of the TA anomaly technique to estimate coral calcification has been repeated many times and is well established (Smith and Kinsey., 1978; Tambutte, E., et al., 1995).

The pH-O₂ method addresses the shortcomings of the pH-TA method wherein discrete samples are needed to be analyzed for TA. The pH-O₂ method was introduced by Barnes (1983) as a means to calculate continuous calcification rates and not be limited by discrete time intervals from TA data. The pH-O₂ method uses relationships between ΔO_2 , ΔDIC_{org} (net community production), and metabolic quotients to estimate net community production and respiration from changes in the concentration of DO. ΔDIC_{org} is calculated by subtracting ΔDIC_{calc} (changes in DIC from calcification) from the total ΔDIC . Metabolic quotients are calculated from net community photosynthesis ($\Delta O_2/\Delta DIC_{org}$) and respiration ($\Delta DIC_{org}/\Delta O_2$). The change in TA and net community calcification are estimated by using the stoichiometric relationships given in Equation 11.

The pH-O₂ method is very attractive because instruments today have very precise and reliable sensors to monitor pH and DO in the field. However, a major drawback of the pH-O₂ method is that it requires the use of assumed values like O₂:CO₂ ratios to calculate the metabolic quotient. The assumptions used to calculate specific metabolic quotients introduce uncertainty to the calculated metabolic parameters.

This method was not chosen for this experiment because of the uncertainty that comes with assuming a specific metabolic quotient for a community. Any biochemical process that yields a ratio of O₂:CO₂ that is stoichiometrically different from the assumed metabolic quotient complicates the pH-O₂ method. This can be seen from the nitrification equation where 2 moles of O₂ are used per mole of NH₄⁺ nitrified (Equation 13).

4.2 – Calculation of Net Ecosystem Calcification Rates

A simple box model (Figure 14) was created to represent the TA of the flow through system setup for this experiment. F_1 represents the TA input flux of the system while F_2 represents the TA output flux. Calcification and dissolution, are processes that contribute to the change in TA at discrete times. F_1 for the control tanks corresponds to the flux of total alkalinity associated with the source water from Kaneohe Bay. This TA fluctuates slightly with time (Figure 11). The total alkalinity flux (F_1) for the experimental tanks is reduced due to the addition of dilute HCl to raise the $p\text{CO}_2$ of the system. Net ecosystem calcification (NEC) calculations are utilized to quantify calcification rates of both control and experimental tanks.

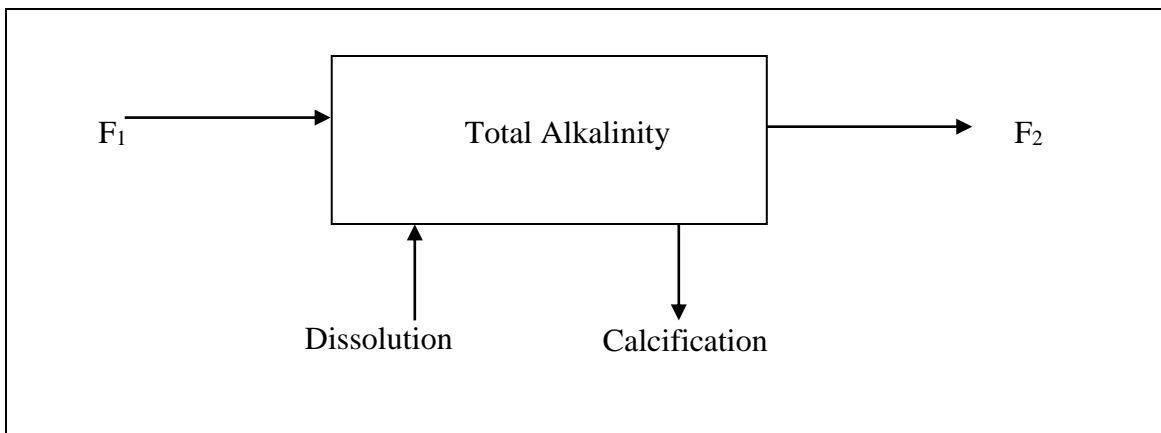


Figure 14. Total alkalinity box model of the ocean acidification experiment. Total alkalinity of the system is the algebraic summation of F_1 , F_2 , calcification and dissolution. F_1 represents the flux of TA in the input solution. F_2 represents the flux of TA leaving the system. The box model is used to calculate the NEC of both the control and experimental tanks. Calcification or dissolution can be calculated by subtracting the sum of F_1 and F_2 from the total change in alkalinity; a positive value denotes calcification while a negative value denotes dissolution.

NEC is used to quantify the difference in calcification rates of the control tanks with ambient pCO₂ levels, as compared to the experimental tanks with elevated pCO₂ levels. The NEC is calculated using Equation 15. F₁ and F₂ are subtracted from the total change in alkalinity of the system. The result is then divided by two to get the calcification, or dissolution rate of the system. A positive value for the result means calcification is occurring while a negative value means there is net dissolution.

$$\text{NEC } (\mu\text{mol/hr}) = [\text{dTA/dt } (\mu\text{mol/hr}) - F_2 (\mu\text{mol/hr}) + F_1 (\mu\text{mol/hr})] / 2 \quad (15)$$

dTA/dt represents the change in TA of the system with respect to time. This is calculated using Equation 16.

$$\text{dTA/dt } (\mu\text{mol/hr}) = [\text{TA}_{\text{time1}} (\mu\text{mole/Kg}) - \text{TA}_{\text{time2}} (\mu\text{mole/Kg})] / 4 (\text{hrs}) \times 500 (\text{Kg}) \quad (16)$$

The difference between TA_{time1} and TA_{time2} is divided by 4 hours to account for TA measurements that were taken in 4-hour time intervals, and then multiplied by 500 Kg to account for the mass of the water in the tank. F₁ represents the input TA flux of the system. Equation 17 is used to calculate the F₁ for the control tanks.

$$F_1 (\mu\text{mol/hr}) = (\text{flowrate}_{\text{tank}} (\text{Kg/hr})) \times [(\text{TA}_{\text{input}(\text{time2})} (\mu\text{mol/Kg}) + \text{TA}_{\text{input}(\text{time1})} (\mu\text{mole/Kg})) / 2] \quad (17)$$

F₁ is calculated by multiplying the flow rate of the tank by the average TA of the input tank between time 1 and time 2. The TA input flux has to be corrected for the experimental tanks wherein dilute acid is added. The F₁ for the experimental tank is represented by equation 18.

$$F_{1 \text{ exp}} (\mu\text{mol/hr}) = (\text{flowrate}_{\text{tank}} (\text{Kg/hr})) \times [(\text{TA}_{\text{input}(\text{time}2)}(\mu\text{mol/Kg}) + \text{TA}_{\text{input}(\text{time}1)}(\mu\text{mol/Kg}))/2] - \text{acid addition} (\mu\text{mol/Kg}) \quad (18)$$

The addition of acid ($\mu\text{mol/hr}$) is subtracted from the flow rate of the experimental tank because it removes TA from the system. The acid addition is represented by Equation 19.

$$\text{Acid Addition} (\mu\text{mol/hr}) = (\text{pump speed} (\text{Kg/hr})) \times (\text{H}^+ \text{ concentration} (\mu\text{mol/kg})) \quad (19)$$

F_2 ($\mu\text{mol/hr}$) is calculated by multiplying the average TA between time 1 and time 2 in both the control and experimental tanks by the flow rate ($\mu\text{mol/hr}$). This is represented in Equation 20.

$$F_2 (\mu\text{mol/hr}) = (\text{flowrate}_{\text{tank}} (\text{Kg/hr})) \times [(\text{TA}_{\text{tank}(\text{time}2)}(\mu\text{mol/Kg}) + \text{TA}_{\text{tank}(\text{time}1)}(\mu\text{mol/Kg}))/2] \quad (20)$$

The combination of equations 15 to 20 allows for the calculation of the NEC of the system. Factors in the natural system that were not accounted for in calculating NEC include gas exchange between the atmosphere and seawater in the tank, and evaporation.

4.3 – Discussion of results

The NEC values are shown in Figure 15. The blue symbols represent the control tanks (tanks 8, 10, 12), while the red symbols represent the experimental tanks (tanks 7, 9, 11). As expected, calcification rates are noticeably lower for the experimental tanks.

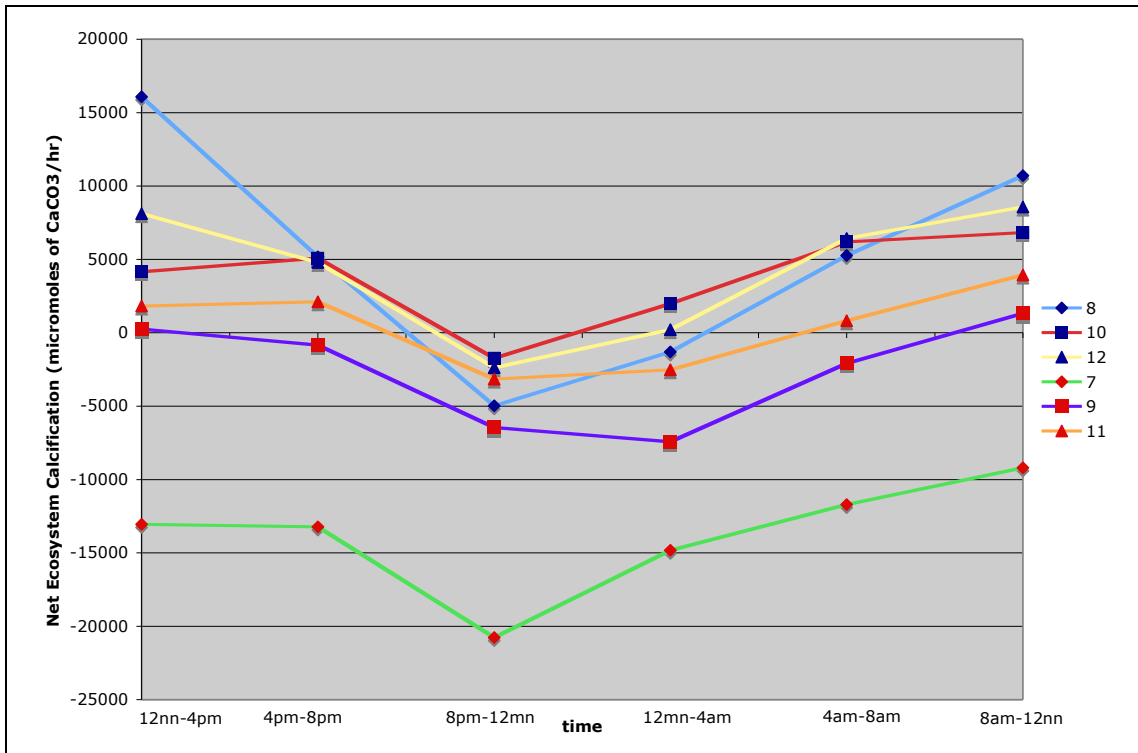


Figure 15. Net ecosystem calcification (NEC) rates throughout the 24-hour ocean acidification experiment. All the control tanks (blue) show calcification during the day, and dissolution at night. This is what is expected in natural systems. Only tank 7 of the experimental tanks shows constant dissolution, however the NEC values of the experimental tanks are generally lower than those of the control tanks. Tank 8 of the control tanks reached a dissolution rate similar to the range of experimental tanks between 8 pm to 12 mn.

Figure 15 shows the NEC results for the ocean acidification experiment. The control tanks (blue) show calcification during the day, and dissolution at night. This is what is expected in natural systems because of photosynthesis and respiration. NEC rates for experimental tanks (red) are interesting in that the trends are the same as those of the control tanks; however, these tanks display a much lower rate of calcification during the day, and higher dissolution rates at night. This indicates that although calcification still occurs at CO₂ levels of >700ppmv, dissolution at night exceeds calcification during the day which means a net dissolution occurs during a 24-hour cycle. Figure 16 shows this trend more clearly. The average of all control tanks (blue bars) shows calcification

throughout the day, and dissolution at night when respiration exceeds photosynthesis. The average of all experimental tanks shows dissolution throughout the day. Although this scenario is more likely to occur in natural systems slowly, perhaps allowing the corals to adapt, the significant difference in NEC of the experimental tanks as compared to the control tanks provides strong evidence for concluding that coral NEC will change significantly under rising CO₂ levels.

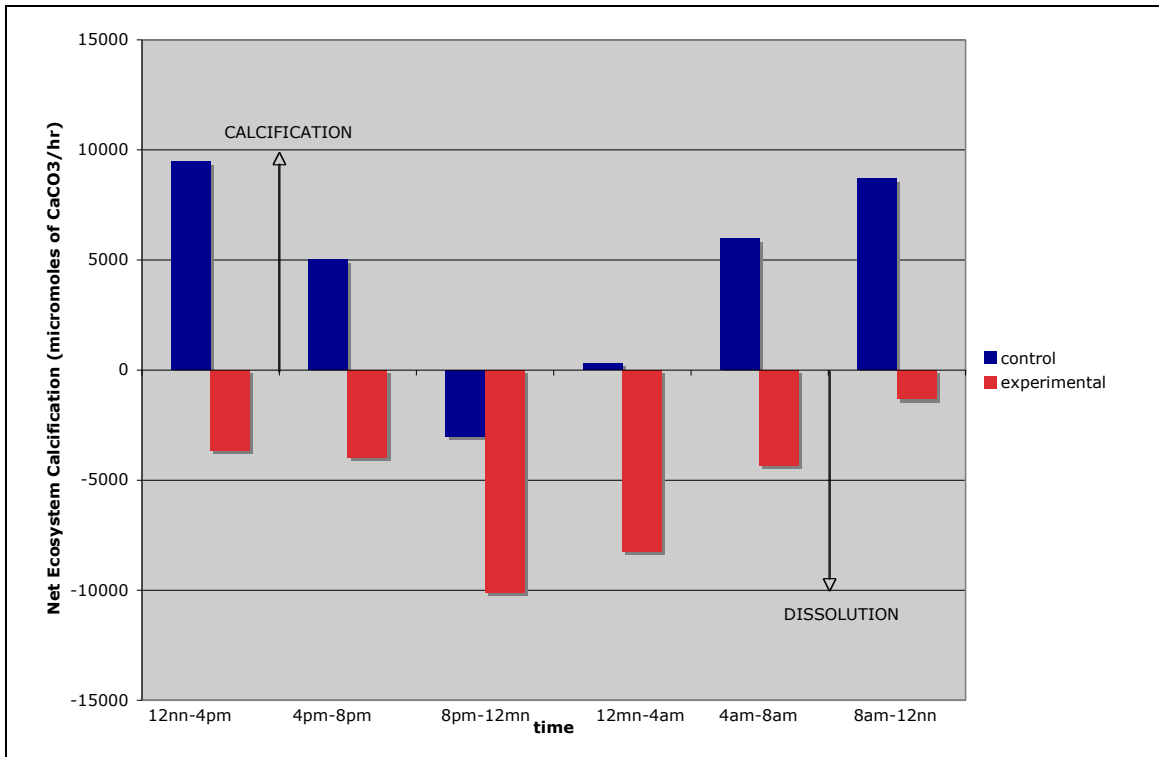


Figure 16. Average net ecosystem calcification rates throughout the 24-hour ocean acidification experiment (NEC). Average NEC for control tanks (blue) and experimental tanks (red) show more clearly that a higher pCO₂ in the future will lead to dramatic changes in calcification rates. The increase in pCO₂ in the experimental tank was enough to halt net ecosystem calcification throughout the day.

A 2-tailed t test was conducted to determine whether a significant change in calcification rates by corals due to the increased CO₂ in the system is present. Based on the mean and standard deviation of the calcification rates between the tanks with ambient and increased CO₂ levels, the statistical test yielded a value of 4.0408. Since this value is

greater than the critical t at 10 degrees of freedom and 95% level of significance of 2.228, the conclusion is that the differences between control and experimental tanks are significant, and that a 24 hour cycle appears to be sufficient to induce a dramatic change in coral calcification.

Chapter 5 – Conclusions

Earth system science is a very broad and interdisciplinary field. The study of it is a culmination of different research, from numerous fields, focusing on different issues. Understanding the different mechanisms of earth sciences, and identifying its implications will always be an ongoing process. This research only touched the surface of a very broad, complex, and extensive issue, which is ocean acidification brought about by global warming. Data gathered from this experiment are only part of the larger picture of ocean acidification.

There are many causes for the rise of atmospheric CO₂. Both natural and anthropogenic factors play a role in the addition of CO₂ to the atmosphere. The main concern is the anthropogenic CO₂ that is being added to the atmosphere, and more specifically the rate at which this is happening. The burning of fossil fuels and oxidation of terrestrial biosphere from deforestation play the major role in the annual increase of pCO₂ in the atmosphere. Over the past century, the release of CO₂ to the atmosphere from fossil fuel burning alone accounts for most of the CO₂ increase in the atmosphere (Mackenzie, 2003). This is a real concern because as the partial pressure of CO₂ in the atmosphere increases, the amount of CO₂ absorbed by the ocean also increases. As discussed earlier, this changes the equilibrium of the DIC system. The addition of CO₂ to the aqueous solution of the ocean leads to a more acidic ocean.

It has been proposed that metastable carbonate minerals such as Mg-calcite, which is unstable compared to calcite and aragonite, will be an effective buffer to restore

pH and carbonate saturation state (Halley and Yates, 2000). Although this might be a plausible possibility, on short timescales the rates of dissolution are too slow to counter effectively the current increase of atmospheric CO₂ (Kleypas et al., 2006).

The ocean acidification experiment answers a fundamental question relating coral calcification to ocean acidification. This experiment showed that an increase of CO₂ levels to 700 ppm is enough to affect significantly the biogeochemical processes of corals. Data from the experiment clearly show a decrease in calcification rate throughout the diurnal cycle. In natural environments, a decrease in calcification rates favors the success of non-calcifying organisms over calcifying ones (Kuffner et al., in press). As discussed earlier, the process of calcification releases CO₂ generally making coral reefs CO₂ sources to the atmosphere. However, with the decrease in calcification rates, and an increase in production by the non-calcifying organisms, reefs may change into CO₂ sinks rather than sources hence altering the natural global carbon cycle.

This experiment compared the calcification rates of corals grown in mesocosms with an increased CO₂ level (700 ppm) to those of systems with ambient CO₂ levels (380 ppm). Although the change in calcification rates in this experiment is conclusive, natural ecosystems may not immediately show changes of the same degree. This is because atmospheric CO₂ will not increase from 380 ppm to 700 ppm overnight. The slow increase of atmospheric CO₂ probably will decrease calcification rates slowly, perhaps giving corals a chance to cope with the increased stress due to elevated CO₂ levels.

The more immediate concern in terms of coral reef destruction is erosion. Since calcareous organisms are the major reef builders, a decline in calcification rates due to

ocean acidification, together with a constant rate of erosion from both biological and physical agents, may result in a faster and unsustainable degree of erosion for reefs.

The ocean acidification experiment was done using one coral species monitored for 24 hours at elevated CO₂ levels. Further research is necessary to obtain a more definitive correlation between ocean acidification and calcification rates in natural ecosystems. Future experiments of this nature should be done with a more diverse coral community, at longer timescales.

Appendix A – Special Report on Emission Scenarios (SRES)

THE EMISSION SCENARIOS OF THE IPCC SPECIAL REPORT ON EMISSION SCENARIOS (SRES)¹⁷

A1. The A1 storyline and scenario family describes a future world of very rapid economic growth, global population that peaks in mid-century and declines thereafter, and the rapid introduction of new and more efficient technologies. Major underlying themes are convergence among regions, capacity building and increased cultural and social interactions, with a substantial reduction in regional differences in per capita income. The A1 scenario family develops into three groups that describe alternative directions of technological change in the energy system. The three A1 groups are distinguished by their technological emphasis: fossil-intensive (A1FI), non-fossil energy sources (A1T) or a balance across all sources (A1B) (where balanced is defined as not relying too heavily on one particular energy source, on the assumption that similar improvement rates apply to all energy supply and end use technologies).

A2. The A2 storyline and scenario family describes a very heterogeneous world. The underlying theme is self-reliance and preservation of local identities. Fertility patterns across regions converge very slowly, which results in continuously increasing population. Economic development is primarily regionally oriented and per capita economic growth and technological change more fragmented and slower than other storylines.

B1. The B1 storyline and scenario family describes a convergent world with the same global population, that peaks in mid-century and declines thereafter, as in the A1 storyline, but with rapid change in economic structures toward a service and information economy, with reductions in material intensity and the introduction of clean and resource-efficient technologies. The emphasis is on global solutions to economic, social and environmental sustainability, including improved equity, but without additional climate initiatives.

B2. The B2 storyline and scenario family describes a world in which the emphasis is on local solutions to economic, social and environmental sustainability. It is a world with continuously increasing global population, at a rate lower than A2, intermediate levels of economic development, and less rapid and more diverse technological change than in the B1 and A1 storylines. While the scenario is also oriented towards environmental protection and social equity, it focuses on local and regional levels.

An illustrative scenario was chosen for each of the six scenario groups A1B, A1FI, A1T, A2, B1 and B2. All should be considered equally sound.

The SRES scenarios do not include additional climate initiatives, which means that no scenarios are included that explicitly assume implementation of the United Nations Framework Convention on Climate Change or the emissions targets of the Kyoto Protocol.

(Solomon et al., 2007)

Appendix B: DATA: Measurements from Ocean Acidification Experiment

Date	Tank #	TA(μ mole/Kg)	pH	T ($^{\circ}$ C)	S (SU)	DO (μ mole/Kg)
6/22/10 12:00	7	2019.535	8.06	27.8	35.1	8.38
6/22/10 14:00	7		8.08	28.2		8.54
6/22/10 16:00	7	2075	7.97	27	35.3	7.55
6/22/10 18:00	7		7.9	26.6		6.86
6/22/10 20:00	7	2072.792	7.78	26.3	35.4	6.05
6/22/10 22:00	7		7.73	26		6.06
6/23/10 0:00	7	2111.232	7.77	26	35.4	6.1
6/23/10 2:00	7		7.76	26		6.11
6/23/10 4:00	7	2086.545	7.71	25.8	35.4	6.04
6/23/10 6:00	7		7.66	25.5		6.02
6/23/10 8:00	7	2077.986	7.87	26	35.4	7.15
6/23/10 10:00	7		8	27		7.93
6/23/10 12:00	7	2054.831	8.08	27.7	35.3	8.31
<hr/>						
6/22/10 12:00	8	2102.231	8.28	27.8	35.1	9.15
6/22/10 14:00	8		8.27	28.2		9.19
6/22/10 16:00	8	2120.205	8.2	27	35.1	7.95
6/22/10 18:00	8		8.12	26.6		7
6/22/10 20:00	8	2188.666	7.99	26.3	35.2	5.81
6/22/10 22:00	8		7.93	26		5.63
6/23/10 0:00	8	2218.95	7.92	26	35.2	5.61
6/23/10 2:00	8		7.92	26		5.64
6/23/10 4:00	8	2209.051	7.88	25.8	35.3	5.59
6/23/10 6:00	8		7.85	25.5		5.62
6/23/10 8:00	8	2176.666	8.06	26	35.2	7.34
6/23/10 10:00	8		8.21	27		8.59
6/23/10 12:00	8	2145.093	8.28	27.6	35.3	8.91
<hr/>						
6/22/10 12:00	9	1947.756	7.93	27.8	35.1	8.11
6/22/10 14:00	9		7.91	28.2		8.13
6/22/10 16:00	9	2007.916	7.82	26.9	35.2	7.41
6/22/10 18:00	9		7.77	26.5		6.83
6/22/10 20:00	9	2011.018	7.66	26.3	35.2	6.13
6/22/10 22:00	9		7.61	26		6.19
6/23/10 0:00	9	2039.015	7.63	26	35.2	6.14
6/23/10 2:00	9		7.64	25.9		6.23
6/23/10 4:00	9	2055.645	7.58	25.8	35.3	6.12
6/23/10 6:00	9		7.55	25.4		6.14
6/23/10 8:00	9	2020.637	7.74	26	35.3	7.2
6/23/10 10:00	9		7.88	27.1		7.9
6/23/10 12:00	9	1999.628	7.94	27.7	35.2	8.18

Date	Tank #	TA(μmoles/Kg)	pH	T (°C)	S (SU)	DO (μmoles/Kg)
6/22/10 12:00	10	2111.676	8.19	27.9	35	8.62
6/22/10 14:00	10		8.19	28.4		8.71
6/22/10 16:00	10	2175.404	8.15	27.1	35.2	7.81
6/22/10 18:00	10		8.1	26.6		6.97
6/22/10 20:00	10	2167.775	8	26.3	35.2	5.99
6/22/10 22:00	10		7.96	26		5.98
6/23/10 0:00	10	2207.465	7.98	25.9	35.2	5.97
6/23/10 2:00	10		7.97	25.9		6.02
6/23/10 4:00	10	2194.014	7.94	25.8	35.2	5.9
6/23/10 6:00	10		7.88	25.4		5.9
6/23/10 8:00	10	2172.658	8.04	26	35.3	7.21
6/23/10 10:00	10		8.16	27.1		8.15
6/23/10 12:00	10	2162.531	8.2	27.8	35.2	8.52
6/22/10 12:00	11	1965.004	7.87	27.7	35	7.95
6/22/10 14:00	11		7.85	28.1		7.99
6/22/10 16:00	11	1992.766	7.79	26.9	35.2	7.4
6/22/10 18:00	11		7.72	26.5		6.8
6/22/10 20:00	11	1997.644	7.62	26.2	35.2	6.1
6/22/10 22:00	11		7.58	26		6.16
6/23/10 0:00	11	2023.277	7.61	25.9	35.2	6.12
6/23/10 2:00	11		7.61	25.9		6.2
6/23/10 4:00	11	2031.514	7.56	25.7	35.2	6.06
6/23/10 6:00	11		7.51	25.4		6.08
6/23/10 8:00	11	2010.346	7.7	25.9	35.2	7.13
6/23/10 10:00	11		7.83	27		7.74
6/23/10 12:00	11	1986.742	7.89	27.5	35.2	7.91
6/22/10 12:00	12	2107.295	8.23	27.7	35	8.97
6/22/10 14:00	12		8.22	28.1		8.99
6/22/10 16:00	12	2151.519	8.18	26.9	35.2	7.86
6/22/10 18:00	12		8.12	26.4		6.88
6/22/10 20:00	12	2174.748	7.99	26.2	35.2	5.84
6/22/10 22:00	12		7.93	25.9		5.82
6/23/10 0:00	12	2209.542	7.94	25.9	35.2	5.8
6/23/10 2:00	12		7.94	25.9		5.85
6/23/10 4:00	12	2203.951	7.9	25.7	35.3	5.75
6/23/10 6:00	12		7.88	25.4		5.76
6/23/10 8:00	12	2168.021	8.05	25.9	35.2	7.37
6/23/10 10:00	12		8.17	27		8.56
6/23/10 12:00	12	2152.353	8.24	27.6	35.2	8.83
6/22/10 12:00	i1	2163.207	8.07	27	35	6.99
6/22/10 14:00	i1		8.06	27.1		7.05
6/22/10 16:00	i1	2200.516	8.06	26.8	35.2	7.04
6/22/10 18:00	i1		8.08	26.9		6.73
6/22/10 20:00	i1	2185.946	8.03	26.7	35.2	6.59
6/22/10 22:00	i1		8.04	26.5		6.5
6/23/10 0:00	i1	2196.364	8.05	26.5	35.2	6.5
6/23/10 2:00	i1		8.04	26.5		6.5
6/23/10 4:00	i1	2215.863	7.94	26	35.1	6.11
6/23/10 6:00	i1		7.97	25.9		6.12
6/23/10 8:00	i1	2196.46	8.07	26.3	35.2	6.59
6/23/10 10:00	i1		8.09	26.7		6.73
6/23/10 12:00	i1	2196.998	8.09	26.9	35.1	6.86

Appendix C: Calculations for NEC

$$dTA/dt (\mu\text{moles/hour}) = [(TA_{1200} (\mu\text{moles/Kg}) - TA_{1600} (\mu\text{moles/Kg}) / 4] \times 500 (\text{Kg})$$

Tank #	12nn-4pm	4pm-8pm	8pm-12mn	12mn-4am	4am-8am	8am-12nn
8	-2246.75	-8557.625	-3785.5	1237.375	4048.125	3946.625
10	-7966	953.625	-4961.25	1681.375	2669.5	1265.875
12	-5528	-2903.625	-4349.25	698.875	4491.25	1958.5
7	-6933.125	276	-4805	3085.875	1069.875	2894.375
9	-7520	-387.75	-3499.625	-2078.75	4376	2626.125
11	-3470.25	-609.75	-3204.125	-1029.625	2646	2950.5

Tank #	flow rate (Kg/hr)			
	Kg	seconds	Kg/min	Kg/hr
8	18	133	8.1203007	487.2180
10	17.6	149	7.087248	425.2348
12	17.3	150	6.92	415.2
7	17.6	128	8.25	495
9	17.5	137	7.664233	459.8540
11	17.8	140	7.628571	457.7142

$$F1 (\mu\text{moles/hr}) = (\text{flowrate of tank (Kg/hr)}) \times [(TA_{\text{input}1600} (\mu\text{moles/Kg}) + TA_{\text{input}1200} (\mu\text{moles/Kg})) / 2]$$

Tank #	12nn-4pm	4pm-8pm	8pm-12mn	12mn-4am	4am-8am	8am-12nn
8	1063042.295	1068581.72	1067570.256	1074858.307	1074881.693	1070286.009
10	927803.6553	932638.3635	931755.5758	938116.4521	938136.8634	934125.8352
12	905908.8948	910629.5112	909767.556	915978.3252	915998.2548	912081.8808

acid addition ($\mu\text{mole/hr}$) = (pump speed) \times (H⁺ conc) \times (per hour) = $((1.3 \times 10^{-3} \text{ Kg/min}) \times 1.1 \text{ mol/Kg} \times 60 \text{ min/hr}) \times 10^6$
 exp tanks 85800

$$F1_{\text{exp}} (\mu\text{moles/hr}) = (\text{tank flowrate (Kg/hr)}) \times [(TA_{\text{input}1600} (\mu\text{moles/Kg}) + TA_{\text{input}1200} (\mu\text{moles/Kg})) / 2] - \text{acid addition}$$

Tank #	12nn-4pm	4pm-8pm	8pm-12mn	12mn-4am	4am-8am	8am-12nn
7	994221.4425	999849.345	998821.725	1006226.183	1006249.943	1001580.855
9	917537.7701	922766.0803	921811.4234	928690.1496	928712.2226	924374.6496
11	912869.178	918073.1606	917122.9457	923969.6649	923991.6351	919674.2451

$$F2 (\mu\text{moles/hr}) = (\text{flowrate of tank (Kg/hr)}) \times [(TA_{\text{tank}1600} (\mu\text{moles/Kg}) + TA_{\text{tank}1200} (\mu\text{moles/Kg})) / 2]$$

Tank #	12nn-4pm	4pm-8pm	8pm-12mn	12mn-4am	4am-8am	8am-12nn
8	1028623.507	1049679.853	1073735.026	1078700.995	1068400.232	1052819.486
10	911508.0161	923435.6424	930252.3705	935831.2397	928430.6642	921736.829
12	884129.7864	898133.0292	910178.604	916241.1468	907621.3872	896909.6424
7	1013397.413	1026578.52	1035545.94	1038949.808	1030721.423	1022872.208
9	909515.8248	924061.4672	931211.9672	941472.9197	937247.3212	924367.5
11	905763.9343	913233.8314	920216.4917	927967.8831	925008.5314	914762.1394

$$\text{NEC } (\mu\text{moles/hr}) = (\text{dTA/dt } (\mu\text{moles/hr}) + \text{F1}(\mu\text{moles/hr}) - \text{F2}(\mu\text{moles/hr}))/2$$

Tank #	12nn-4pm	4pm-8pm	8pm-12mn	12mn-4am	4am-8am	8am-12nn
8	16086.01898	5172.121335	-4975.134	-1302.656	5264.793327	10706.57415
10	4164.819597	5078.173037	-1729.0223	1983.293674	6187.849597	6827.440587
12	8125.5542	4796.4285	-2380.149	218.0267	6434.0588	8565.3692
7	-13054.5475	-13226.5875	-20764.6075	-14818.875	-11700.8025	-9198.48875
9	250.9726277	-841.5684	-6450.084	-7430.7600	-2079.54927	1316.637318
11	1817.496857	2114.789571	-3148.8355	-2513.921	814.5518571	3931.302857
	avg NEC					
	4pm-12nn	8pm-4pm	12mn-8pm	4am-12mn	8am-4am	12nn-8am
control	9458.797594	5015.57429	-3028.102	299.5545045	5962.233908	8699.794647
experimental	-3662.026	-3984.455	-10121.1758	-8254.518	-4321.933	-1316.849

References

- Anderson, A.J., 2003. Climate Change and Anthropogenic Effects on Shallow-Water Carbonate Biogeochemistry, Masters Thesis, University of Hawaii.
- Anderson, A.J., and Mackenzie, F.T., 2004. Shallow-water oceans: a source or sink of atmospheric CO₂? *Front Ecol Environ.* 2(7): 348-353.
- Anderson, A.J., Mackenzie, and F.T., Ver, L.M., 2003. Solution of shallow-water carbonates: An insignificant buffer against rising atmospheric CO₂. *Geology*, 31: 513-516.
- Archer, D. (1996) A data-driven model of the global calcite lysocline. *Global Biogeochem. Cycles*, 10, 511-526.
- Archer, D., Kheshgi, H., and Maier-Reimer, E. (1998) Dynamics of fossil fuel CO₂ neutralization by marine CaCO₃. *Global Biogeochem. Cycles*, 12, 259-276.
- Barnes, D.J. (1983) *J. Exp. Mar. Biol. Ecol.* 66, 149-161.
- Barnes, D., and Cuff, C., 2000. Solution of reef rock buffers seawater against rising atmospheric pCO₂, in Hopley, D., Hopley, M. Tاملندر, J., Done, T., Proceedings of the Ninth International Coral Reef Symposium Abstracts, State Ministry for the Environment, Indonesia, pp248
- Barnola, J.M., Raynaud, D., Lorius, and C., Barkov, N.I., 2003. Historical CO₂ record from the Vostok ice core. In *Trends: A Compendium of Data on Global Change. Carbon Dioxide Information Analysis Center, Oak Ridge National Laboratory, U.S. Department of Energy, Oak Ridge, Tenn., U.S.A.*
- Brennan, S.T., Lowenstein, T.K., and Horita, J. (2004) Seawater chemistry and the advent of biocalcification. *Geology*, 32, 473-476.
- Cai, W.J. and Wang, Y. (1998) The chemistry, fluxes, and sources of carbon dioxide in the estuarine waters of the Satilla and Altamaha Rivers, Georgia. *Limnol. Oceanogr.* 43, 657-668.
- Chisholm, J.R.M., and Gattuso, J.-P. (1991) Validation of the alkalinity anomaly technique for investigating calcification of photosynthesis in coral reef communities. *Limnol. Oceanogr.* 36, 1232-1239.
- DOE, 1994. Handbook of methods for the analysis of the various parameters of the carbon dioxide system in sea water; version 2. Dickinson, A.G., and Goyet, C., eds., ORNL/CDIAC-74.

Emerson, S., and Bender, M.L., 1981. Carbon fluxes at the sediment-water interface of the deep sea: calcium carbonate preservation, *J. Mar. Res.* 39, 139-162.

Frankignoulle, M., Canon, C., and Gattuso, J.-P. (1994) Marine calcification as a source of carbon dioxide: Positive feedback of increasing atmospheric CO₂. *Limnol. Oceanogr.* 39, 458-462.

Friis-Christensen, and E., Lassen, K., 1991. Length of the solar cycle: an indicator of solar activity closely associated with climate. *Science*, 254: 698-700.

Gattuso, J.-P., Frankignoulle, M., Bourge, I., Romaine, S., and Buddemeier, R.W., 1998. Effect of calcium carbonate saturation of sea water on coral calcification. *Global Planetary Change*, 18:37-46.

Gattuso, J.-P., Frankignoulle, M., and Smith, S.V. (1999) Measurement of community metabolism and significance in the coral reef CO₂ source-sink debate. *Proc. Nat. Acad. Sci. US*, 96, 13, 017-13, 022.

Halley, R.B., and Yates, K.K., 2000. Will reef sediments buffer corals from increased global CO₂, in Hopley, D., Hopley, M., Tamelander, J., and Done, T., *Proceedings of the Ninth International Coral Reef Symposium Abstracts*, State Ministry for the Environment, Indonesia, p. 248.

Houghton, J.T., Ding, Y., Griggs, D.J., Noguer, M., van der Linden, P.J., Dai, X., Maskell, K., and Johnson, C.A., 2001. *Climate Change 2001: The scientific basis. Contribution of Working Group I to the third Assessment Report of the Intergovernmental Panel on Climate Change*: Cambridge, Cambridge University Press, 881 p.

Houghton, J.T., Meiro Filho, L.G., Callander, B.A., Harris, N., Kattenberg, A., and Maskell, K., 1996. *Climate change 1995: The science of climate change. Contribution of working group I to the Second Assessment Report of the Intergovernmental Panel on Climate Change*, Cambridge University Press, 572 p.

IPCC, 2007. *Climate Change 2007: The Physical Science Basis. Contribution of Working Group I to the Fourth Assessment Report of the Intergovernmental Panel on Climate Change* [Solomon, S., D. Qin, M. Manning, Z. Chen, M. Marquis, K.B. Averyt, M. Tignor and H.L. Miller (eds.)]. Cambridge University Press, Cambridge, United Kingdom and New York, NY, USA.

Kinsey, D.W. (1978) Alkalinity changes and coral reef calcification. *Limnol. Oceanogr.* 28, 568-574.

Kleypas, J.A., Feely, R.A., Fabry, V.J., Langdon, C., Sabine, C.L., and Robbins, L.L., 2006. Impacts of Ocean Acidification on Coral Reefs and Other Marine Calcifiers: A Guide for Future Research. A report from a workshop sponsored by the National Science Foundation, the National Oceanic and Atmospheric Administration, and the U.S. Geological Survey.

Kuffner, I.B., Andersson, A.J., Jokiela, P.L., Rodgers, K., and Mackenzie, F.T., in press. Potential impact of future ocean acidification on crustose coralline algal recruitment and growth. *Nature*.

Lerman, A., and Mackenzie, F.T., 2005. CO₂ Air-sea exchange due to calcium carbonate and organic matter storage, and its implications for the global carbon cycle, *Aquatic Geochemistry*, 11:345-390.

Lewis, E., and Wallace, D.W.R., 1998. Program Developed for CO₂ System Calculations. ORNL/CDIAC-105: Carbon Dioxide Information Analysis Center, Oak Ridge National Laboratory, U.S. Department of Energy, Oak Ridge, Tennessee.

Mackenzie, F.T., and Agegian, C.R., 1989. Biomineralization and tentative links to plate tectonics, in Crick, R.E., *Origin, Evolution, and Modern Aspects Biomineralization in Plants and Animals*: New York, Plenum Press, p. 11-27.

Mackenzie, F.T., 2003. *Our Changing Planet: An Introduction to Earth System Science and Global Environmental Change*. Pearson Education, Inc. Upper Saddle River, New Jersey.

Mehrbach, C., Culbertson, C.H., Hawley, J.E., and Pytkowicz, R.M., 1973. Measurement of the apparent dissociation constants of carbonic acid in seawater at atmospheric pressure. *Limnology and Oceanography*, 18, 897-907.

Morse, J.W., and Mackenzie, F.J., 1990. *Geochemistry of Sedimentary Carbonates, Developments in Sedimentology 48*. Elsevier, N.Y. 707 pp.

Morse, J.W., Andersson, A.J., and Mackenzie, F.J., 2006. Initial responses of carbon-rich shelf sediments to rising atmospheric pCO₂ and "ocean acidification": Role of high Mg-calcites. *Geochim. et Cosmochim. Acta*, 70, 5814-5834.

Peng, T.H., Takahashi, T., Broecker, W.S., and Olafsson, J., 1987. Seasonal variability of carbon dioxide, nutrients and oxygen in the northern North Atlantic surface water: Observations and model. *Tellus* 39B, 439-458.

Petit, J.R., Jouzel, J., Reynaud, D., Barkov, N.I., Barnola, J.M., Basile, I., Benders, M., Chappellaz, J., Davis, M., Delaygue, G., Delmotte, M., Kotlyakov, V.M., Legrand, M., Lipenkov, V.Y., Lorius, C., Pepin, L., Ritz, C., Saltzman, E., and Stievenard, M., 1999. Climate and atmospheric history of the past 420,000 years from the Vostok ice core, Antarctica. *Nature*, 399: 429-436.

Pilson, M.E., 1998. An Introduction to the Chemistry of the Sea. Prentice Hall, Upper Saddle River, NJ, 431p.

Prentice, I.C. and others (2001) The carbon cycle and atmospheric CO₂, p. 183-287. In J.T. Houghton and D. Yihui, Climate Change: The Scientific Basis, Contribution of working group I to the Third Assessment Report of the Intergovernmental Panel on Climate Change, Cambridge University Press.

Rodgers K., Jokiel P.L., Coz, E.F., Andersson, A.J., Kuffner, I.B., and Farrell, F., in press. The potential impacts of ocean acidification on reproduction in the scleractinian coral *Montipora capitata*.

Sabine C.L., Freely, R.A., Gruber, N., Key, R.M., Lee, K., Bullister J.L., Wanninkhof R., Wong, C.S., Wallace, D.W.R., Tilbrook, B., Milerio, F.J., Peng, T.H., Kozyr, A., Ono, T., and Rios, A.F., 2004. The oceanic sink for anthropogenic CO₂. Science, 305: 367-371

Sarmiento, J.L., Hughes, T.M.C., Stouffer, R.J., and Manabe, S. (1998) Simulated response of the ocean carbon cycle to anthropogenic climate warming. Nature, 393, 245-249.

Siegenthaler, U., and Sarmiento, J.L., 1993. Atmospheric carbon dioxide and the ocean. Nature, 365, 119-125.

Siegenthaler, U., Stocker, T.F., Monnin, E., Lüthi, D., Schwander, J., Stauffer, B., Raynaud D., Barnola, J.M., Fischer, H., Masson-Delmotte, V., and Jouzel, J., 2005. Stable carbon cycle–climate relationship during the Late Pleistocene. Science, Vol. 310. no. 5752, pp. 1313 - 1317

Smith, S.V., and Kinsey, D.W., 1978. Coral Reefs: Research Methods, eds. Stoddart, D.R. & Johannes, R.E. (UNESCO, Paris), pp. 469-484.

Solomon, S., D. Qin, M. Manning, R.B. Alley, T. Berntsen, N.L. Bindoff, Z. Chen, A. Chidthaisong, J.M. Gregory, G.C. Hegerl, M. Heimann, B. Hewitson, B.J. Hoskins, F. Joos, J. Jouzel, V. Kattsov, U. Lohmann, T. Matsuno, M. Molina, N. Nicholls, J. Overpeck, G. Raga, V. Ramaswamy, J. Ren, M. Rusticucci, R. Somerville, T.F. Stocker, P. Whetton, R.A. Wood and D. Wratt, 2007: Technical Summary. In: Climate Change 2007: The Physical Science Basis. Contribution of Working Group I to the Fourth Assessment Report of the Intergovernmental Panel on Climate Change [Solomon, S., D. Qin, M. Manning, Z. Chen, M. Marquis, K.B. Averyt, M. Tignor and H.L. Miller (eds.)]. Cambridge University Press, Cambridge, United Kingdom and New York, NY, USA.

Svensmark, H., 1998. Influence of cosmic rays on Earth's climate. Physical Review Letters, 81: 5027-5030.

Tambutte, E., Allemand, D., Bourge, I., Gattuso, J.-P., and Jaubert, J.,1995. *Mar. Biol.* 122, 453-459.

Ware, J.R., Smith, S.V., and Reaka-Kudla, M.L., 1992. Coral reefs: Sources or sinks of atmospheric CO₂? *Coral reefs*, 11:127-130.